To the Graduate Council:

I am submitting herewith a thesis written by John Paul McMillan, Jr. entitled " Effects of Fiber Volume Fraction on the Elastic Stability of Specially Orthotropic Plates." I have examined the final copy of this thesis for form and content and recommend that it be accepted in partial fulfillment of the requirements for the degree of Master of Science, with a major in Aerospace Engineering.

Dr. Gary Flandro, Major Professor

We have read this thesis
and recommend its acceptance:

Uwe Peter Solies

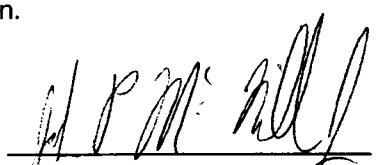
Accepted for the Council:

Associate Vice Chancellor
and Dean of the Graduate School

STATEMENT OF PERMISSION TO USE

In presenting this thesis in partial fulfillment of the requirements for a Master's degree at the University of Tennessee, Knoxville, I agree that the Library shall make it available to borrowers under rules of the Library. Brief quotations from this thesis are allowable without special permission, provided that accurate acknowledgement of the source is made.

Permission for extensive quotation from or reproduction of this thesis may be granted by my major professor, or in his absence, by the head of Interlibrary Services when, in the opinion of either, the proposed use of the material is for scholarly purposes. Any copying or use of the material in this thesis for financial gain shall not be allowed without my written permission.

Signature 

Date April 27, 1994

EFFECTS OF FIBER VOLUME FRACTION ON THE ELASTIC STABILITY OF SPECIALLY ORTHOTROPIC PLATES

A Thesis

Presented for the

Master of Science

Degree

The University of Tennessee, Knoxville

John Paul McMillan, Jr.

May 1994

DEDICATION

To Gabriel, Seth, and Grace

ACKNOWLEDGEMENTS

I would like to thank my major professor, Dr. Gary Flandro, for his valuable guidance and assistance in completing this work. I would also like to thank the other members of my committee, Dr. Ching Lo and Dr. Peter Solies, for their council and advice over the past few months. Special thanks to Mr. Tom Bailey, who provided the funding I needed this past year, and to Mrs. Mary Lo who tracked down all those books and papers I required to complete this work. Finally, I wish to express my gratitude to my parents, Paul and Shirley McMillan, and my sister, Marilyn Creech, and her family, for all the support they have given me over the many years.

ABSTRACT

This paper presents an analysis of the effects of fiber volume fraction on the elastic stability of composite plates. Specially orthotropic boron-epoxy plates having various fiber volume fractions and plate geometries are examined in detail. Only the case of in-plane compressive loads is considered. The analysis is done using a computer program that calculates both the material properties and buckling loads of the plates. Micromechanics theory is used first to calculate the physical properties of the plates for the various fiber volume fractions. The buckling loads are then calculated by an equation derived from Reissner's Variational Theorem. This buckling equation accounts for transverse shear deformation, which can significantly affect the buckling loads of composite plates. Results of the analysis show that fiber volume fraction is a considerable factor in a composite plate's ability to withstand buckling. It is concluded that increasing the fiber content of a composite material, within reasonable limits, will enhance the elastic stability of composite plates.

TABLE OF CONTENTS

CHAPTER PAGE

1. INTRODUCTION 1

2. PROPERTIES OF SPECIALLY ORTHOTROPIC LAMINAE 3
   - Introduction and Nomenclature 3
   - Stress-Strain Relations 4
   - Engineering Constants and the Compliance Matrix 8

3. DETERMINATION OF LAMINA PROPERTIES FROM CONSTITUENT PROPERTIES 12
   - Introduction 12
   - Prediction of the Longitudinal Properties of a Lamina 13
   - Prediction of the Transverse Properties of a Lamina 16

4. ELASTIC STABILITY OF SPECIALLY ORTHOTROPIC PLATES 21
   - Introduction 21
   - Assumptions of Plate Theory 22
   - Reissner's Variational Theorem 24
   - Development of the Buckling Equation 28

5. EFFECTS OF FIBER VOLUME FRACTION ON PLATE STABILITY 35
   - Introduction 35
   - Analysis 35
   - Results 37

6. CONCLUSIONS AND RECOMMENDATIONS 45

BIBLIOGRAPHY 47

APPENDIX 51

VITA 55

LIST OF TABLES

TABLE PAGE

2-1. Comparison Between Tensor and Contracted Notation for Stresses and Strains 5

2-2. Direction Cosines 7

5-1. Elastic Properties of Constituent Materials 36

5-2. Elastic Properties of Boron-Epoxy Plates 36

5-3. Buckling Loads for Boron-Epoxy Plates 1/4 Inch Thick 41

5-4. Buckling Loads for Boron-Epoxy Plates 1/3 Inch Thick 41

5-5. Buckling Loads for Boron-Epoxy Plates 1/2 Inch Thick 41

5-6. Percentage Change in Buckling Loads for Boron-Epoxy Plates 1/4 Inch Thick 43

5-7. Percentage Change in Buckling Loads for Boron-Epoxy Plates 1/3 Inch Thick 43

5-8. Percentage Change in Buckling Loads for Boron-Epoxy Plates 1/2 Inch Thick 43

LIST OF FIGURES

FIGURE PAGE

2-1. Representative Volume Element of a UDC 4

2-2. Axial Transformation of the x_3 Plane 7

3-1. Representative Volume Element Loaded in the Longitudinal Direction 14

3-2. Representative Volume Element Depicting Poisson's Effects 16

3-3. Representative Volume Element Loaded in the Transverse Direction 18

4-1. Rectangular Plate 22

5-1. Buckling Load vs. Aspect Ratio for Boron-Epoxy Plates 1/4 Inch Thick 38

5-2. Buckling Load vs. Aspect Ratio for Boron-Epoxy Plates 1/3 Inch Thick 39

5-3. Buckling Load vs. Aspect Ratio for Boron-Epoxy Plates 1/2 Inch Thick 40

5-4. Percentage Change in Buckling Load vs. Volume Fraction 44

NOMENCLATURE

A_{mn}	Variational Constant
a, A	Plate edge length in x-direction
b, B	Plate edge length in y-direction
A/B	Aspect ratio (length/width)
C_{ij}, S_{ij}	Stiffness and compliance matrices
D_x, D_y	Flexural rigidity
E_1, E_x	Longitudinal Young's modulus
E_2, E_y	Transverse Young's modulus
E_3, E_z	Transverse Young's modulus
E_f, E_m	Young's modulus of fibers and matrix
G_{12}, G_{xy}	Shear modulus in longitudinal-transverse plane
G_{13}, G_{xz}	Shear modulus in longitudinal-vertical plane
G_{23}, G_{yz}	In-plane shear modulus
G_f, G_m	Shear modulus of fibers and matrix
h	Plate thickness
m, n	Longitudinal and transverse buckling modes
M_x, M_y, M_{xy}	Stress couples
N_x, N_y	In-plane loads
Q_x, Q_y	Transverse shear resultants
u, v	Displacements in the x and y directions
V_f	Volume fraction
W	Strain energy density function
w	Lateral displacement in z-direction
α, β	Rotations in the x and y directions

ϵ_{ij}, σ_{ij}	Strain and stress tensors
ν_{12}, ν_{xy}	Major Poisson's ratio
ν_{21}, ν_{yx}	Minor Poisson's ratio
ν_{23}, ν_{yz}	In-plane Poisson's ratio
ν_f, ν_m	Fiber and matrix Poisson's ratio
ψ	Reissner's functional

CHAPTER 1

INTRODUCTION

Consider a composite plate subjected to an in-plane compressive load. If the plate remains in stable equilibrium it will retain its flat condition. If the load exceeds a particular value, however, the plate will become unstable and deform from its original shape. Such a plate has buckled, and the compressive force that caused the deformation is called the buckling load.

Plate geometry, fiber and matrix type, and the ability of the matrix to support the fibers under compression all influence a composite plate's ability to withstand buckling. Another parameter influencing a composite plate's elastic stability is its fiber volume fraction. Fiber volume fraction represents the percentage of a composite's total volume occupied by the reinforcement filaments. The purpose of this paper is to examine what effects the fiber volume fraction have on the buckling load of a composite plate.

In this analysis, a series of unidirectional composite plates made of boron-epoxy is examined. Each plate is considered simply supported on the x-edges and clamped on the y-edges. A uniform compressive load is applied to the x-edges. The plates are varied in thickness, aspect ratio (length/width), and fiber volume fraction. Buckling loads for the plates are obtained from the computer program listed in the Appendix. Comparisons of plates with similar geometries are made to analyze how varying the fiber volume fraction alters the buckling loads.

The physical properties of each plate are determined from the properties of the constituent materials and their relative volumetric percentages. Typical values of engineering constants for boron fiber and epoxy resin are used to calculate the elastic moduli and

Poisson's ratios of the composite plates. The plates' engineering constants are determined by the computer program using the rule of mixtures and the Halpin-Tsai equations.

Reissner's Variational Theorem, the Theorem of Minimum Potential Energy, and the Rayleigh-Ritz method are used to develop the governing equation for the buckling load (Smith, 1973). Transverse shear deformation, which is generally neglected in classical, linear, thin-plate theory, is accounted for in this equation. Including the effects of transverse shear deformation can, in many instances, significantly increase the accuracy of the buckling loads obtained (Vinson & Chou, 1975).

Comparisons of buckling loads for each system of plates are shown in graphical form. Percentage increases in buckling loads for each plate are compared to correspondent increases in fiber volume fraction.

Results of the analysis show that raising the fiber volume fraction of a composite plate significantly increases its elastic stability. The fiber reinforcements effectiveness to withstand compressive loads is also shown to increase at the higher fiber volume fractions.

CHAPTER 2

PROPERTIES OF SPECIALLY ORTHOTROPIC LAMINAE

Introduction and Nomenclature

An unidirectional fiber composite (UDC) consists of continuous fibers embedded in a matrix material, such as epoxy resin. Figure 2-1 is a representative volume element of such a UDC. If the fibers are aligned so that the principal material axes and the natural body axes of the lamina are the same, the composite is termed specially orthotropic. In other words, the composite has mutually perpendicular axes of symmetry in its longitudinal and transverse directions.

In general, the distribution of fibers over a given cross section of a UDC is sufficiently random so that no preferential direction of reinforcement is provided for in any transverse plane (Rosen & Dow, 1987). Specially orthotropic composites can therefore be treated as transversely isotropic.

In this chapter, the elastic parameters required to analyze a specially orthotropic lamina will be determined. Hooke's Law will be used to derive the stiffness matrix that defines the stress-strain relations of the composite material. The components of the strain-stress relations, or compliance matrix, will then be translated into their equivalent engineering constants. Only those constants required for analyzing a UDC will be retained.

Stress-Strain Relations

The functional relationship between the stress and strain of an elastic body is the generalized Hooke's Law. In tensor notation, Hooke's law is expressed mathematically as

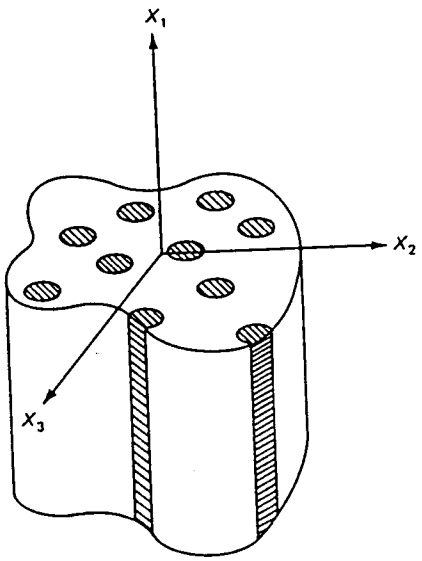


Figure 2-1. Representative Volume Element of a UDC.

Source: Rosen, "Analysis of Material Properties," Engineered Materials Handbook, Volume 1, Composites, ASM International, Third Printing, August, 1989.

$$\sigma_{ij} = C_{ijkl}\,\epsilon_{kl} \qquad [i,j,k,l = 1,2,3] \quad (2.1)$$

where σ_{ij} and ϵ_{kl} are the second-order stress and strain tensors, and C_{ijkl} is the fourth-order elasticity tensor. From Eq.(2.1) it is observed that C_{ijkl} contains 81 elastic constants. Since σ_{ij} and ϵ_{kl} are both symmetric, however, C_{ijkl} can be reduced from 81 to 36 constants. Hooke's Law can now be written in the contracted notation

$$\sigma_i = C_{ij}\,\epsilon_j \qquad [i,j = 1,2,...,6] \quad (2.2)$$

Table 2-1 relates the tensor notation of the stresses and strains to its contracted form.

C_{ij} represents the stiffness matrix of an elastic body and contains 36 constants. If it is assumed that an elastic potential, or strain energy density function, exists then C_{ij} may be reduced to 21 independent elastic constants. Such an elastic potential will exist if the variation

TABLE 2-1. Comparison Between Tensor and Contracted Notation for Stresses and Strains.

STRESSES		STRAINS	
Tensor Notation	Contracted Notation	Tensor Notation	Contracted Notation
σ_{11}	σ_1	ϵ_{11}	ϵ_1
σ_{22}	σ_2	ϵ_{22}	ϵ_2
σ_{33}	σ_3	ϵ_{33}	ϵ_3
$\tau_{23}=\sigma_{23}$	σ_4	$\gamma_{23}=2\epsilon_{23}$*	ϵ_4
$\tau_{31}=\sigma_{31}$	σ_5	$\gamma_{31}=2\epsilon_{31}$	ϵ_5
$\tau_{12}=\sigma_{12}$	σ_6	$\gamma_{12}=2\epsilon_{12}$	ϵ_6

* Note that γ_{ij} ($i \neq j$) represents engineering shear strain whereas ϵ_{ij} ($i \neq j$) represents tensor shear strain.

Source: Jones, Mechanics of Composite Materials, Scripta Book Company, 1975.

of the body under deformation occurs isothermally, that is, the temperature of each element remains constant (Lekhnitskii, 1963). It can be shown by differentiating the strain energy density function (e.g., see Jones, 1975) that the stiffness matrix is symmetric, i.e., $C_{ij} = C_{ji}$, and the total number of independent constants is 21. The resultant stiffness matrix represents the general form for an anisotropic material, and is expressed

$$[C_{ij}] = \begin{bmatrix} C_{11} & C_{12} & C_{13} & C_{14} & C_{15} & C_{16} \\ C_{12} & C_{22} & C_{23} & C_{24} & C_{25} & C_{26} \\ C_{13} & C_{23} & C_{33} & C_{34} & C_{35} & C_{36} \\ C_{14} & C_{24} & C_{34} & C_{44} & C_{45} & C_{46} \\ C_{15} & C_{25} & C_{35} & C_{45} & C_{55} & C_{56} \\ C_{16} & C_{26} & C_{36} & C_{46} & C_{56} & C_{66} \end{bmatrix} \tag{2.3}$$

Orthotropic materials exhibit properties of elastic symmetry along orthogonal planes. If the direction of the axis perpendicular to a plane of symmetry is reversed, the elastic constants will remain the same (Agarwal & Broutman, 1990). This invariance to axial transformations allows Eq. (2.3) to be reduced to nine independent elastic constants.

As an example, consider a plane of symmetry in the x_1-x_2 plane. Figure 2-2 represents a transformation such that $x_1 = x'_1$, $x_2 = x'_2$, and $x_3 = -x'_3$ Table 2-2 relates the corresponding direction cosines. The stresses and strains of the original coordinate system are related to the new system by the tensor transformations

$$\begin{aligned} \sigma'_{mn} &= a_{mk} a_{nl} \sigma_{kl} \\ \epsilon'_{mn} &= a_{mk} a_{nl} \epsilon_{kl} \end{aligned} \tag{2.4}$$

Expanding Eqs.(2.4) gives $\sigma_{23} = -\sigma'_{23}$, $\sigma_{31} = -\sigma'_{31}$, $\epsilon_{23} = -\epsilon'_{23}$, and $\epsilon_{31} = -\epsilon'_{31}$. All of the other stresses and strains are equal.

If Eq.(2.2) is expanded, and the results of Eqs.(2.4) are input for the primed and

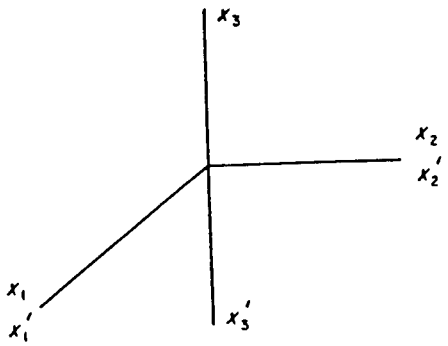


Figure 2-2. Axial Transformation of the x_3 Plane.

Source: Vinson & Chou, Composite Materials and Their Use in Structures, John Wiley & Sons, 1975.

Table 2-2. Direction Cosines.

	x_1	x_2	x_3
x'_1	$a_{11}=1$	$a_{12}=0$	$a_{13}=0$
x'_2	$a_{21}=0$	$a_{22}=1$	$a_{23}=0$
x'_3	$a_{31}=0$	$a_{32}=0$	$a_{33}=-1$

unprimed stresses and strains, the invariance condition requires that certain constants of C_{ij} equal zero. These are

$$C_{14} = C_{15} = C_{24} = C_{25} = C_{34} = C_{35} = C_{46} = C_{56} = 0$$

A similar analysis of the x_2-x_3 plane requires

$$C_{16} = C_{26} = C_{36} = C_{45} = 0$$

Analyzing the x_1-x_3 plane produces no further reductions, and so the stiffness matrix for an orthotropic material becomes

$$[C_{ij}] = \begin{bmatrix} C_{11} & C_{12} & C_{13} & 0 & 0 & 0 \\ C_{12} & C_{22} & C_{23} & 0 & 0 & 0 \\ C_{13} & C_{23} & C_{33} & 0 & 0 & 0 \\ 0 & 0 & 0 & C_{44} & 0 & 0 \\ 0 & 0 & 0 & 0 & C_{55} & 0 \\ 0 & 0 & 0 & 0 & 0 & C_{66} \end{bmatrix} \qquad (2.5)$$

Engineering Constants and the Compliance Matrix

To evaluate a composite material in terms of its physical properties, it is necessary to transform the elasticity constants into equivalent engineering constants. The conversion is simplified if the stress-strain relationship of Eq.(2.2) is first inverted into the strain-stress relationship

$$\epsilon_i = S_{ij}\sigma_j \qquad [i,j = 1,...,6] \qquad (2.6)$$

where S_{ij}, the compliance matrix, is the inverse of C_{ij}. Since C_{ij} is symmetric, its inverse S_{ij} is

symmetric also. The compliance matrix is expressed

$$[S_{ij}] = \begin{bmatrix} S_{11} & S_{12} & S_{13} & 0 & 0 & 0 \\ S_{12} & S_{22} & S_{23} & 0 & 0 & 0 \\ S_{13} & S_{23} & S_{33} & 0 & 0 & 0 \\ 0 & 0 & 0 & S_{44} & 0 & 0 \\ 0 & 0 & 0 & 0 & S_{55} & 0 \\ 0 & 0 & 0 & 0 & 0 & S_{66} \end{bmatrix} \tag{2.7}$$

Expanding Eq.(2.6) produces the following set of strain-stress equations:

$$\begin{aligned} \epsilon_1 &= S_{11}\sigma_1 + S_{12}\sigma_2 + S_{13}\sigma_3 \\ \epsilon_2 &= S_{12}\sigma_1 + S_{22}\sigma_2 + S_{23}\sigma_3 \\ \epsilon_3 &= S_{13}\sigma_1 + S_{23}\sigma_2 + S_{33}\sigma_3 \\ \epsilon_4 &= S_{44}\sigma_4 \\ \epsilon_5 &= S_{55}\sigma_5 \\ \epsilon_6 &= S_{66}\sigma_6 \end{aligned} \tag{2.8}$$

The components of the compliance matrix can now be translated into engineering constants by a series of simple tensile tests and pure shear tests (Vinson & Chou, 1975). Since the material is specially orthotropic, normal stresses applied along the material axes will only produce normal strains and shear stresses will only produce shear strains (Agarwal & Broutman, 1990).

Consider a single stress, σ_1, applied to the material in the x_1 direction. With all the other stresses set to zero, Eqs.(2.8) reduce to:

$$\begin{aligned} \epsilon_1 &= S_{11}\sigma_1 = \sigma_1/E_1 \\ \epsilon_2 &= S_{12}\sigma_1 = -\nu_{12}\epsilon_1 = -\nu_{12}\sigma_1/E_1 \\ \epsilon_3 &= S_{13}\sigma_1 = -\nu_{13}\epsilon_1 = -\nu_{13}\sigma_1/E_1 \end{aligned} \tag{2.9}$$

where E_1 is the longitudinal modulus of elasticity and ν_{12} and ν_{13} are Poisson's ratios.

Therefore

$$\begin{aligned} S_{11} &= 1/E_1 \\ S_{12} &= -\nu_{12}/E_1 \\ S_{13} &= -\nu_{13}/E_1 \end{aligned} \tag{2.10}$$

Similar tests in the x_2 and x_3 planes, with σ_2 and σ_3 the respective stresses give

$$\begin{aligned} S_{12} &= -\nu_{21}/E_2 \\ S_{22} &= 1/E_2 \\ S_{23} &= -\nu_{23}/E_2 \end{aligned} \tag{2.11}$$

and

$$\begin{aligned} S_{13} &= -\nu_{31}/E_3 \\ S_{23} &= -\nu_{32}/E_3 \\ S_{33} &= 1/E_3 \end{aligned} \tag{2.12}$$

where E_2 and E_3 are the transverse moduli of elasticity.

Comparing Eqs.(2.10 - 2.12) reveals an important reciprocal relationship

$$\frac{\nu_{ij}}{E_i} = \frac{\nu_{ji}}{E_j} \tag{2.13}$$

Any parameter in Eq.(2.13) can be easily determined if the other three are known.

The three remaining compliance constants of Eqs.(2.8) are transformed by a pure shear test applied to each orthogonal plane. Results of the shear test yields

$$S_{44} = 1/G_{23}$$
$$S_{55} = 1/G_{13} \qquad (2.14)$$
$$S_{66} = 1/G_{12}$$

where G_{23}, G_{13}, and G_{12} are the moduli of rigidity.

Collecting terms, the engineering constants required to analyze specially orthotropic materials are E_1, E_2, E_3, G_{12}, G_{13}, G_{23}, ν_{12}, ν_{13}, ν_{21}, ν_{23}, ν_{31}, and ν_{32}. If the material is transversely isotropic in the x_2-x_3 plane, then $E_2 = E_3$, $G_{12} = G_{13}$, $\nu_{12} = \nu_{13}$, $\nu_{21} = \nu_{31}$ and $\nu_{23} = \nu_{32}$. Therefore, the material properties needed to analyze the unidirectional composite plates being considered are E_1, E_2, G_{12}, G_{23}, ν_{12}, ν_{21}, and ν_{23}.

CHAPTER 3

DETERMINATION OF LAMINA PROPERTIES FROM CONSTITUENT PROPERTIES

Introduction

The elastic properties of a UDC are functions of the elastic properties of its fibers and matrix and of their relative volumes in the composite material (Rosen, 1987). This chapter's purpose is to relate these constituent properties to the mechanical behavior of the composite lamina.

Micromechanics is a study of mechanical properties of unidirectional composites in terms of those of constituent materials (Tsai & Hahn, 1980). Two approaches have been taken in the development of micromechanics theory: mechanics of materials and theory of elasticity. In both approaches, a representative volume element is used to model the phase geometry and mechanical behavior of the total composite. The element is statistically homogeneous to the UDC, yet small enough to analyze at the micromechanical level.

Predictions of composite behavior derived from micromechanics theory are highly dependent on the element model chosen. Various solutions have been determined using several models and experimental data can be found to support almost any result (Christensen, 1979). Although no absolute consensus exists about the results of micromechanics theory, there is wide acceptance of certain approximations which have been applied in practical composite design. These approximations are the rule of mixtures and the Halpin-Tsai equations. For purposes of this analysis, these micromechanics formulas will be used to determine the mechanical behavior of the composite plates.

Prediction of the Longitudinal Properties of a Lamina

Longitudinal properties of a UDC may be predicted from either the mechanics of materials or elasticity approach. The mechanics of materials approach is more elementary but requires an assumption concerning either the stress or strain distribution over the cross-section (Calcote, 1969). This approach leads to the rule of mixtures for the longitudinal Young's modulus, E_1, and the major Poisson's ratio, ν_{12}.

The elasticity theory approach uses variational methods to establish upper and lower bounds for E_1 and ν_{12}. Although the elasticity approach is more rigorous in its development, its solutions are not significantly different from the rule of mixtures. Generally, the rule of mixtures solutions are accepted as good approximations to those of elasticity theory. Therefore, the simpler mechanics of materials approach will be used here to derive E_1 and ν_{12}.

Consider the representative volume element shown in Figure 3-1. If the fibers and matrix are assumed to be perfectly bonded, then the strains in the composite, fibers, and matrix will be equal:

$$\epsilon_c = \epsilon_f = \epsilon_m \tag{3.1}$$

Assuming that both the fibers and matrix are elastic allows the stresses to be expressed as

$$\begin{aligned} \sigma_f &= E_f \epsilon_f \\ \sigma_m &= E_m \epsilon_m \end{aligned} \tag{3.2}$$

Let σ_1 be the average stress acting on the cross-section, A, of the element. The load P causing the stress can then be written

$$P = \sigma_1 A = \sigma_f A_f + \sigma_m A_m \tag{3.3}$$

where $\sigma_f A_f$ and $\sigma_m A_m$ equal the portion of the load carried by the fibers and matrix.

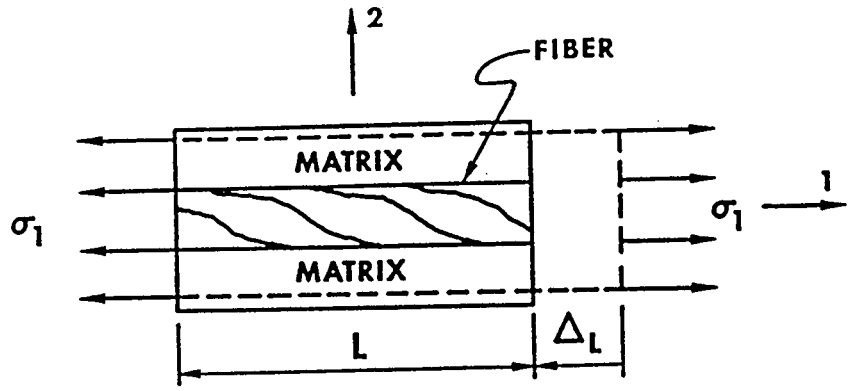


Figure 3-1. Representative Volume Element Loaded in the Longitudinal Direction.

Source: Jones, Mechanics of Composite Materials, Scripta Book Co., 1975.

Substituting Eqs.(3.2) into Eq.(3.3), and rewriting σ_1 as

$$\sigma_1 = E_1 \epsilon_c \tag{3.4}$$

gives

$$E_1 \epsilon_c = E_f \epsilon_f \frac{A_f}{A} + E_m \epsilon_m \frac{A_m}{A} \tag{3.5}$$

If the fibers run parallel throughout the element, then the volume fractions of the fibers and matrix, V_f and V_m, will equal the area fractions

$$V_f = \frac{A_f}{A} \quad , \quad V_m = \frac{A_m}{A} \tag{3.6}$$

Substituting Eqs.(3.6) into Eq.(3.5) and using the equality of Eq.(3.1) yields

$$E_1 = E_f V_f + E_m V_m \tag{3.7}$$

Eq.(3.7) is known as the rule of mixtures and represents the longitudinal Young's modulus of the composite element.

The major Poisson's ratio, ν_{12}, relates longitudinal strain to transverse strain. It is defined as

$$\nu_{12} = -\frac{\epsilon_2}{\epsilon_1} \tag{3.8}$$

Figure 3-2 depicts the transverse contraction caused by a longitudinal stress. Let W equal the initial width of the element and Δw equal the transverse deformation. Then, ϵ_2, the transverse strain is

$$\epsilon_2 = -\frac{\Delta w}{W} = -\nu_{12}\epsilon_1 \tag{3.9}$$

Solving Eq.(3.9) for Δw gives

$$\Delta w = \nu_{12}\epsilon_1 W \tag{3.10}$$

Now let Δw equal the sum of the fiber and matrix deformations, $\Delta_f w$ and $\Delta_m w$, such that

$$\Delta w = \Delta_f w + \Delta_m w \tag{3.11}$$

Approximations for $\Delta_f w$ and $\Delta_m w$ in terms of their volume fractions are

$$\begin{aligned} \Delta_f w &= V_f \nu_f \epsilon_1 W \\ \Delta_m w &= V_m \nu_m \epsilon_1 W \end{aligned} \tag{3.12}$$

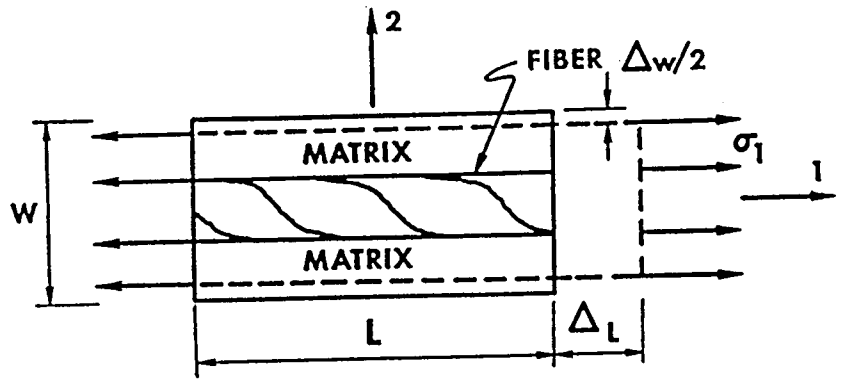


Figure 3-2. Representative Volume Element Depicting Poisson's Effects..

Source: Jones, Mechanics of Composite Materials, Scripta Book Co., 1975.

Combining Eqs.(3.10), (3.11), & (3.12) gives

$$\nu_{12}\epsilon_1 W = V_f \nu_f \epsilon_1 W + V_m \nu_m \epsilon_1 W \tag{3.13}$$

Solving for ν_{12} results in

$$\nu_{12} = V_f \nu_f + V_m \nu_m \tag{3.14}$$

Eq.(3.14) is the rule of mixtures for the major Poisson's ratio. The minor Poisson's ratio, ν_{21}, can be determined from ν_{12} using the reciprocal relationship of Eq.(2.13).

Prediction of the Transverse Properties of a Lamina

A mechanics of materials approach to predicting a UDC's transverse properties is based on assumptions that are inconsistent. This approach requires one to assume that the transverse stress and longitudinal Poisson effects are the same in both the fibers and the

matrix material. Figure 3-3 depicts a representative volume element loaded in the transverse direction. It is not likely, however, that the constituent materials will experience either the same transverse stress or the same longitudinal Poisson-effect deformation (Calcote, 1969). Therefore, an elasticity approach must be used to predict a composite material's transverse properties.

Formal elasticity approaches to micromechanics can be classified into variational methods, exact methods, and self-consistent model methods. All these methods result in complicated equations and/or curves which are either awkward to use or limited to a few available cases (Jones, 1975). A solution to this difficulty would be a set of simple, generalized equations that accurately approximate the more complicated micromechanical results. Such equations have been developed by Halpin and Tsai who were able to show that Herman's solution generalizing Hill's self-consistent model can be reduced to an approximate form (Halpin, 1984). The predictions of the Halpin-Tsai equations are quite accurate if the fiber volume fraction does not approach one (Agarwal & Broutman, 1990).

The Halpin-Tsai equations are expressed as

$$\frac{p}{p_m} = \frac{(1 + \zeta \eta V_f)}{(1 - \eta V_f)} \tag{3.15}$$

where

$$\eta = \frac{(\frac{p_f}{p_m} - 1)}{(\frac{p_f}{p_m} + \zeta)} \tag{3.16}$$

The quantities p, p_f, p_m, and ζ are identified as:

p = composite moduli, E_2 or G_{12};

p_f = corresponding fiber modulus, E_f or G_f respectively;

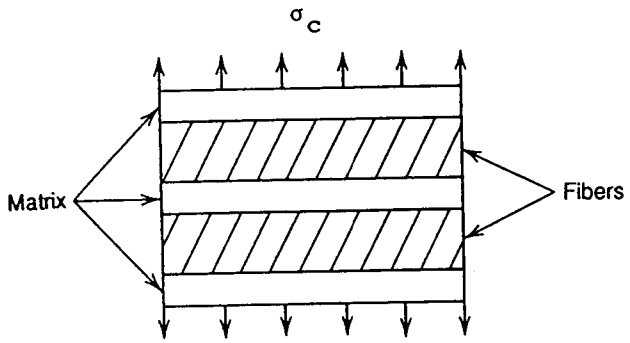


Figure 3-3. Representative Volume Element Loaded in the Transverse Direction.

Source: Agarwal & Broutman, Analysis and Performance of Fiber Composites, Second Edition, John Wiley & Sons, Inc., 1990.

p_m = corresponding matrix modulus, E_m or G_m;

ζ = a measure of reinforcement which depends on the boundary conditions (Halpin, 1984).

Eq.(3.15) provides a straightforward method for calculating the transverse Young's modulus, E_2, and the shear modulus, G_{12}. The only complication is choosing appropriate values for the ζ factor. Values for ζ are obtained by comparing Eqs.(3.15) & (3.16) with exact elasticity solutions and assessing a value of, or function for, ζ by curve fitting techniques (Jones, 1975). Halpin and Tsai compared their equations with Adams and Donner's numerical results for circular fibers in a square array. As a result, they suggested values of $\zeta = 1$ for G_{12} and $\zeta = 2$ for E_2.

It has been pointed out that the Halpin-Tsai equations yield underestimates to the square array results for higher fiber volume fractions (Hewitt & Malherbe, 1970). Hewitt and Maljerbe have shown a better approximation for the ζ factor for G_{12} to be

$$\zeta_{G_{12}} = 1 + 40V_f^{10} \tag{3.17}$$

Based on this work, Halpin modified the original approximations for ζ to

$$\zeta_{G_{12}} = 1 + 40V_f^{10} \tag{3.18}$$

$$\zeta_{E_2} = 2 + 40V_f^{10} \tag{3.19}$$

Using Eqs.(3.18) & (3.19) together with the Halpin-Tsai equations yields engineering estimates for E_2 and G_{12} which are quite accurate for fiber volume fractions up to 0.75 .

The last material property required for analyzing composite laminae is the in-plane shear modulus, G_{23}. For composites which can be characterized as transversely isotropic, G_{23} can be computed from the simple expression

$$G_{23} = \frac{E_2}{2(1 + \nu_{23})} \tag{3.20}$$

once E_2 and ν_{23} are determined (Pagano & Tsai, 1968). Eq. (3.20) is analogous to the expression for the shear modulus of isotropic materials. An approximation for ν_{23} is

$$\nu_{23} \cong \frac{(1 - \eta_G)(1 + \eta_E\zeta_E)}{(1 - \eta_E)(1 + \eta_G\zeta_G)}\frac{E_m}{2G_m} - 1 \tag{3.21}$$

where ζ_G and ζ_E are Eqs.(3.18) and (3.19) and η_G and η_E are Eq.(3.16) using ζ_G and ζ_E respectively (Halpin, 1984).

All of the necessary equations to determine the elastic properties of an unidirectional composite lamina in terms of its constituents have been derived. In summary, these are:

E_1	Eq.(3.7)
ν_{12}	Eq.(3.14)
ν_{21}	Eq.(2.13)
E_2, G_{12}	Eq.(3.15)
G_{23}	Eq.(3.20)

These equations are the most generally agreed upon methods for obtaining lamina material properties (Vinson & Chou, 1975).

CHAPTER 4

ELASTIC STABILITY OF SPECIALLY ORTHOTROPIC PLATES

Introduction

Consider the flat, rectangular plate of length a, width b, and thickness h, shown in Figure 4-1 . The plate is referenced to an xyz Cartesian coordinate system where the upper and lower surfaces are z = h/2 and -h/2 respectively. The plate is specially orthotropic, therefore, its material axes, 1-2-3, coincide with the xyz system. N_x and N_y are the compressive loads per unit edge distance applied to the x and y edges respectively.

Let it be assumed that the forces N_x and N_y act on the middle plane of the plate. At some discrete value of these forces the middle plane will undergo some small lateral bending consistent with the given boundary conditions. Such limited bending can be produced without stretching the middle plane, therefore, only the energy due to bending and the work done by the forces need be considered (Timoshenko & Gere, 1961).

Now consider two possible states for the plate. In the first state, the plate is in equilibrium under the compressive forces and the middle plane remains flat. Here, the work done by the forces is less than the strain energy for any possible buckled shape. In the second state, the work done by the forces is larger than the energy of bending and the middle plane is slightly curved. In other words, the plate has become unstable and buckling has occurred.

According to the theory of minimum potential energy, a state of equilibrium will be stable if the potential energy in that state has a minimum value by comparison with any other possible state close to the state of equilibrium (Chen, 1968). Furthermore, at the point where an elastic body transitions from a configuration of equilibrium, prior to buckling, to an

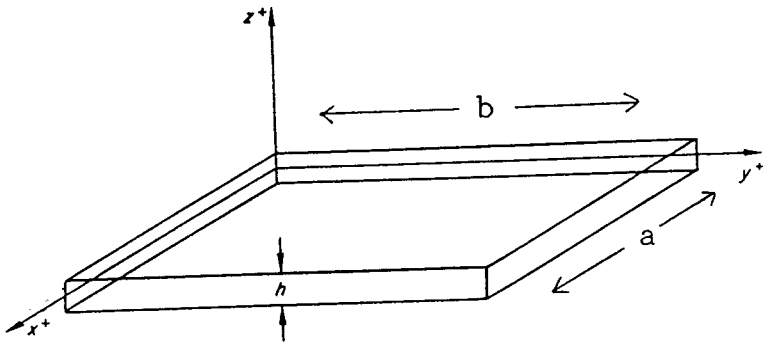


Figure 4-1. Rectangular Plate.

Source: Vinson & Chou, Composite Materials and Their Use in Structures, Halsted Press, 1975.

infinitesimally near adjacent configuration at the initiation of buckling, the change in potential energy is zero (Vinson & Chou, 1975). This principle may be used to develop the governing equation that defines the elastic stability of plates.

In this chapter, Reissner's Variational Theorem is used to develop a general potential energy expression for specially orthotropic plates. The potential energy is then formed in terms of the lateral displacements only. Finally the Rayleigh-Ritz method is used to generate the buckling equation for the case of a plate simply supported on the x-edges and clamped on the y-edges.

Assumptions of Plate Theory

In the classical theory of elasticity, several assumptions are made in order to reduce the equations of elasticity into an eigenvalue problem that can readily be solved. These

assumptions are:

(1) An element of the plate normal to the middle surface of the x-y plane, upon application of a load, will undergo at most a translation and a rotation with respect to the original coordinate system.

(2) The element will remain normal to the deformed middle surface.

(3) A plate resists lateral and in-plane loads by bending, transverse shear deformation, and in-plane action, not through block-like compression or tension in the plate in the thickness direction (Vinson & Chou, 1975).

Assumption (1) implies the following general form for the displacements

$$u = u_0(x,y) + z\,\alpha(x,y)$$
$$v = v_0(x,y) + z\,\beta(x,y)$$
$$w = w(x,y)$$

where u_0 and v_0 are the x-y plane surface displacements of the middle plane and α and β are rotations which are yet to be defined.

Assumption (2) is, in essence, the neglect of transverse shear deformation. For isotropic materials, where the ratio of Young's modulus to shear modulus is on the order of

$$2 \le \frac{E}{G} \le 3$$

the transverse shear deformation is negligible. Composite materials, on the other hand, have a Young's modulus that is many times greater than the transverse shear modulus. For composites

$$20 \le \frac{E_1}{G_{13}} \le 50$$

are typical ratios for practical plates. Therefore, for a given Young's modulus, the plate is very weak in transverse shear resistance, and the effects of transverse shear deformation are significant, and cannot be neglected (Vinson & Chou, 1975).

For this reason, Reissner's theorem is used to develop the buckling equation of the composite plate. The variational theorem does not require Assumption (2) be made to develop the equation. Transverse shear effects are included in the equation, and the accuracy of the solutions are increased.

Reissner's Variational Theorem

Reissner's variational theorem may be stated as follows:

Of all the stress and displacement states satisfying the boundary conditions, those which also satisfy the equilibrium equations and the stress displacement relations correspond to a minimum of the functional ψ defined as,

$$\psi = \int_R H \, dR - \int_R F_i u_i \, dR - \int_{S_t} T_i u_i \, dS \qquad (4.1)$$

where

$H = \sigma_{ij}\epsilon_{ij} - W(\sigma_{ij})$.

R = Volume of the elastic body.

T_i = i th component of the surface traction.

u_i = i th component of the deformation.

F_i = i th component of the body force.

S_t = Portion of the surface on which the stresses are proscribed.

$W(\sigma_{ij})$ = Strain energy function in terms of stresses (Vinson & Chou, 1975).

To formulate Reissner's functional an equation for $H = \sigma_{ij}\epsilon_{ij} - W(\sigma_{ij})$ is first developed. A general expression for the strain energy function (per unit volume) is

$$W = \frac{1}{2}\sigma_{ij}\epsilon_{ij} \tag{4.2}$$

Substituting the strain-stress equations (2.8) into Eq.(4.2) gives an expression for the strain energy in terms of stresses only. For a specially orthotropic material then

$$\begin{aligned} W(\sigma_{ij}) = \frac{1}{2}\Bigg[&\frac{\sigma_x^2}{E_x} + \frac{\sigma_y^2}{E_y} + \frac{\sigma_z^2}{E_z} \\ &- 2\left(\frac{\nu_{xy}}{E_x}\sigma_x\sigma_y + \frac{\nu_{yz}}{E_y}\sigma_y\sigma_z + \frac{\nu_{xz}}{E_x}\sigma_x\sigma_z\right) \\ &+ \frac{\sigma_{yz}^2}{G_{yz}} + \frac{\sigma_{xz}^2}{G_{xz}} + \frac{\sigma_{xy}^2}{G_{xy}}\Bigg] \end{aligned} \tag{4.3}$$

The strain-displacement equations from the theory of elasticity may be used to develop the $\sigma_{ij}\epsilon_{ij}$ term. For the case where deflections are small, these equations are:

$$\begin{aligned} \epsilon_x &= u_{,x} \\ \epsilon_y &= v_{,y} \\ \epsilon_z &= w_{,z} \\ \gamma_{xy} &= v_{,x} + u_{,y} \\ \gamma_{xz} &= w_{,x} + u_{,z} \\ \gamma_{yz} &= w_{,y} + v_{,z} \end{aligned} \tag{4.4}$$

where the commas denote partial differentiation. Now, using Assumption (1), concerning the expressions for the displacements, and Assumption (3), that the plate only undergoes bending, Eqs.(4.4) may be rewritten as:

$$
\begin{aligned}
\epsilon_x &= z\frac{\partial \alpha}{\partial x} \\
\epsilon_y &= z\frac{\partial \beta}{\partial y} \\
\epsilon_z &= \frac{\partial w}{\partial z} = 0 \\
\gamma_{xy} &= z\left[\frac{\partial \beta}{\partial x} + \frac{\partial \alpha}{\partial y}\right] \\
\gamma_{xz} &= \left[\frac{\partial w}{\partial x} + \alpha\right] \\
\gamma_{yz} &= \left[\frac{\partial w}{\partial y} + \beta\right]
\end{aligned}
\tag{4.5}
$$

Substituting Eqs.(4.5) into the $\sigma_{ij}\epsilon_{ij}$ term of the parameter H gives:

$$
\begin{aligned}
\sigma_{ij}\epsilon_{ij} = {} & \sigma_x z\frac{\partial \alpha}{\partial x} + \sigma_y z\frac{\partial \beta}{\partial y} + \sigma_z\frac{\partial w}{\partial z} \\
& + \sigma_{xy} z\left[\frac{\partial \beta}{\partial x} + \frac{\partial \alpha}{\partial y}\right] + \sigma_{xz}\left[\frac{\partial w}{\partial x} + \alpha\right] + \sigma_{yz}\left[\frac{\partial w}{\partial y} + \beta\right]
\end{aligned}
\tag{4.6}
$$

To use Reissner's theorem requires that the stresses of Eqs.(4.3) & (4.6) be known. Since the true stresses are not known exactly, the following expressions given by Reissner are used as approximations to the true stresses:

$$
\begin{aligned}
(\sigma_x, \sigma_y, \sigma_{xy}) &= \frac{12z}{h^3}(M_x, M_y, M_{xy}) \\
(\sigma_{xz}, \sigma_{yz}) &= \frac{3}{2h}\left[1 - \left(\frac{z}{h/2}\right)^2\right](Q_x, Q_y) \\
\sigma_z &= \frac{3p}{4}\left[\frac{2}{3} + \frac{z}{h/2} - \frac{1}{3}\left(\frac{z}{h/2}\right)^3\right]
\end{aligned}
\tag{4.7}
$$

In the case being considered, the lateral load, p, equals zero, therefore, σ_z equals zero. Now, substituting Eqs.(4.7) into Eqs.(4.3) & (4.6) yields the following expression for the parameter H:

$$
\begin{aligned}
H = {} & \frac{12M_x}{h^3}\frac{\partial \alpha}{\partial x}z^2 + \frac{12M_y}{h^3}\frac{\partial \beta}{\partial y}z^2 + \frac{12M_{xy}}{h^3}\left[\frac{\partial \beta}{\partial x} + \frac{\partial \alpha}{\partial y}\right]z^2 \\
& + \frac{3}{2h}\left\{\left[1 - \left(\frac{z}{h/2}\right)^2\right]Q_x\left[\frac{\partial w}{\partial x} + \alpha\right] + \left[1 - \left(\frac{z}{h/2}\right)^2\right]Q_y\left[\frac{\partial w}{\partial y} + \beta\right]\right\} \\
& - \frac{1}{2}\left[\frac{1}{E_x}\left(\frac{12M_x z}{h^3}\right)^2 + \frac{1}{E_y}\left(\frac{12M_{yz}}{h^3}\right)^2 - 2\left(\frac{\nu_{xy}}{E_x}\left(\frac{12z}{h^3}\right)^2 M_x M_y\right)\right. \\
& + \frac{1}{G_{yz}}\left(\frac{3}{2h}\left[1 - \left(\frac{z}{h/2}\right)^2\right]Q_y\right)^2 \\
& + \frac{1}{G_{xz}}\left(\frac{3}{2h}\left[1 - \left(\frac{z}{h/2}\right)^2\right]Q_x\right)^2 \\
& \left. + \frac{1}{G_{xy}}\left(\frac{12M_{xy}z}{h^3}\right)^2\right]
\end{aligned}
\tag{4.8}
$$

The second term in the Reissner functional

$$\int_R F_i u_i \, dR \tag{4.9}$$

represents the body forces acting on the plate. In this case the body forces are neglected and Eq.(4.9) equals zero.

The last term in ψ involving the surface tractions represents the work done by the in-plane, compressive stress resultants N_x and N_y. This term may be expressed as

$$\int_{S_t} T_i u_i \, dS = \frac{1}{2}\int_0^a \int_0^b \left[N_x\left(\frac{\partial w}{\partial x}\right)^2 + N_y\left(\frac{\partial w}{\partial y}\right)^2 \right] dydx \tag{4.10}$$

Eq.(4.10) reflects the work done by the lateral deformations caused when the in-plane loads reach the buckling load, wherein lateral deformations, w(x,y), occur, and there is no stretching or shortening of the plate middle surface (Vinson & Chou, 1975).

The expression for the Reissner functional can now be written as:

$$\psi = \int_0^a \int_0^b \int_{\frac{-h}{2}}^{\frac{h}{2}} H \, dz dy dx - \int_0^a \int_0^b \left[\frac{N_x}{2}\left(\frac{\partial w}{\partial x}\right)^2 + \frac{N_y}{2}\left(\frac{\partial w}{\partial y}\right)^2 \right] dy dx \qquad (4.11)$$

where H is Eq.(4.8). Integrating the first term across the thickness gives the Reissner functional:

$$\begin{aligned} \psi = \int_0^a \int_0^b \Bigg[& -\frac{N_x}{2}\left(\frac{\partial w}{\partial x}\right)^2 - \frac{N_y}{2}\left(\frac{\partial w}{\partial y}\right)^2 + M_x \frac{\partial \alpha}{\partial x} + M_y \frac{\partial \beta}{\partial y} \\ & + M_{xy}\left(\frac{\partial \alpha}{\partial y} + \frac{\partial \beta}{\partial y}\right) + Q_x\left(\alpha + \frac{\partial w}{\partial x}\right) + Q_y\left(\beta + \frac{\partial w}{\partial y}\right) \\ & - \frac{6M_x^2}{E_x h^3} - \frac{6M_y^2}{E_y h^3} - \frac{6M_{xy}^2}{G_{xy} h^3} + \frac{12\nu_{xy}}{E_x h^3} M_x M_y \\ & - \frac{3}{5}\left(\frac{Q_x^2}{G_{xz} h} + \frac{Q_y^2}{G_{yz} h}\right) \Bigg] dy dx \end{aligned} \qquad (4.12)$$

Development of the Buckling Equation

Eq.(4.12) represents a potential energy expression which can be used to determine the buckling loads. Before the Rayleigh method can be employed to obtain these critical load solutions, however, the equation must be manipulated to include only terms involving the deflections in the z-direction (Smith, 1973). This can be accomplished by taking variations with respect to all the variables and setting the results equal to zero. The result of taking these variations is Eq.(4.13). The first two bracketed terms of Eq.(4.13) result from integrating by parts the terms involving variations of the displacements, α, β, and w. These two terms set equal to zero specify the boundary conditions. The remaining bracketed coefficients in the double integral, set equal to zero, represent the Euler-Lagrange Equations of the variational problem.

$$
\begin{aligned}
0 = & \int_0^a \left[-N_y \frac{\partial w}{\partial y} \delta w + M_y \delta \beta + M_{xy} \delta \alpha + Q_y \delta w \right]_0^b dx \\
& + \int_0^b \left[-N_x \frac{\partial w}{\partial x} \delta w + M_x \delta \alpha + M_{xy} \delta \beta + Q_x \delta w \right]_0^a dy \\
& + \int_0^a \int_0^b \left\{ \left[N_x \frac{\partial^2 w}{\partial x^2} + N_y \frac{\partial^2 w}{\partial y^2} - \frac{\partial Q_x}{\partial x} - \frac{\partial Q_y}{\partial y} \right] \delta w \right. \\
& + \left[-\frac{\partial M_{xy}}{\partial y} + Q_x - \frac{\partial M_x}{\partial x} \right] \delta \alpha + \left[-\frac{\partial M_{xy}}{\partial x} + Q_y - \frac{\partial M_y}{\partial y} \right] \delta \beta \\
& + \left[\frac{\partial \alpha}{\partial x} - \frac{12 M_x}{E_x h^3} + \frac{12 \nu_{xy} M_y}{E_x h^3} \right] \delta M_x + \left[\frac{\partial \beta}{\partial y} - \frac{12 M_y}{E_y h^3} + \frac{12 \nu_{yx} M_x}{E_y h^3} \right] \delta M_y \\
& + \left[\frac{\partial \alpha}{\partial y} + \frac{\partial \beta}{\partial x} - \frac{12 M_{xy}}{G_{xy} h^3} \right] \delta M_{xy} + \left[\alpha + \frac{\partial w}{\partial x} - \frac{6}{5} \frac{Q_x}{G_{xz} h} \right] \delta Q_x \\
& \left. + \left[\beta + \frac{\partial w}{\partial y} - \frac{6}{5} \frac{Q_y}{G_{yz} h} \right] \delta Q_y \right\} dy dx
\end{aligned}
\tag{4.13}
$$

The Euler-Lagrange equations can be manipulated to give the following stress couples and shear resultants:

$$
\begin{aligned}
M_x &= D_x \left(\frac{\partial \alpha}{\partial x} + \nu_{yx} \frac{\partial \beta}{\partial y} \right) \\
M_y &= D_y \left(\nu_{xy} \frac{\partial \alpha}{\partial x} + \frac{\partial \beta}{\partial y} \right) \\
M_{xy} &= \frac{G_{xy} h^3}{12} \left(\frac{\partial \alpha}{\partial y} + \frac{\partial \beta}{\partial x} \right) \\
Q_x &= \frac{5 G_{xz} h}{6} \left(\alpha + \frac{\partial w}{\partial x} \right) \\
Q_y &= \frac{5 G_{yz} h}{6} \left(\beta + \frac{\partial w}{\partial y} \right)
\end{aligned}
\tag{4.14}
$$

where

$$D_x = \frac{E_x h^3}{12(1-\nu_{xy}\nu_{yx})}$$
$$D_y = \frac{E_y h^3}{12(1-\nu_{xy}\nu_{yx})} \tag{4.15}$$

Substituting Eqs.(4.14) into Eq.(4.12), and after some extensive algebraic manipulations, results in a potential energy expression in terms of the displacements and the physical properties of the plate. The result is

$$\begin{aligned}\psi = \int_0^a \int_0^b \Bigg\{ & \left(\frac{-N_x}{2} + \frac{5}{12}G_{xz}h\right)\left(\frac{\partial w}{\partial x}\right)^2 + \frac{5}{6}\alpha\frac{\partial w}{\partial x}G_{xz}h \\ & + \left(\frac{-N_y}{2} + \frac{5}{12}G_{yz}h\right)\left(\frac{\partial w}{\partial y}\right)^2 + \frac{5}{6}\beta\frac{\partial w}{\partial y}G_{yz}h \\ & + \frac{D_x}{2}\left(\frac{\partial \alpha}{\partial x}\right)^2 + D_x\nu_{yx}\left(\frac{\partial \alpha}{\partial x}\right)\left(\frac{\partial \beta}{\partial y}\right) + \frac{D_y}{2}\left(\frac{\partial \beta}{\partial y}\right)^2 \\ & + \frac{G_{xy}h^3}{24}\left[\left(\frac{\partial \alpha}{\partial y}\right)^2 + 2\left(\frac{\partial \alpha}{\partial y}\right)\left(\frac{\partial \beta}{\partial x}\right) + \left(\frac{\partial \beta}{\partial x}\right)^2\right] \\ & + \frac{5}{12}G_{xz}h\alpha^2 + \frac{5}{12}G_{yz}h\beta^2 \Bigg\}\, dydx\end{aligned} \tag{4.16}$$

The final step, before the Rayleigh method can be applied, is to express the rotations, α and β, in terms of the lateral deflection, w, so that ψ is in terms of w only. This can be accomplished by reducing the Euler-Lagrange equations from Eq.(4.13) to those of a beam in the x-direction (Smith, 1973). The resulting equations are:

$$N_x\frac{d^2w}{dx^2} - \frac{dQ_x}{dx} = 0$$
$$-\frac{dM_x}{dx} + Q_x = 0 \tag{4.17}$$

$$\frac{d\alpha}{dx} - \frac{12M_x}{E_x h^3} = 0$$

$$\alpha + \frac{dw}{dx} - \frac{6}{5}\frac{Q_x}{G_{xz}h} = 0$$

From Eqs.(4.17) it can be shown that

$$\alpha(x) = \frac{E_x h^2}{10G_{xz}}\frac{d^3w}{dx^3}\left(\frac{6N_x}{5G_{xz}h}-1\right) - \frac{dw}{dx} \tag{4.18}$$

In a similar manner, for a beam in the y-direction

$$\beta(y) = \frac{E_y h^2}{10G_{yz}}\frac{d^3w}{dy^3}\left(\frac{6N_y}{5G_{yz}h}-1\right) - \frac{dw}{dy} \tag{4.19}$$

Eqs.(4.18) & (4.19) can now be generalized for the case of a plate so that

$$\begin{aligned}\alpha(x,y) &= \frac{E_x h^2}{10G_{xz}}\frac{\partial^3 w}{\partial x^3}\left(\frac{6N_x}{5G_{xz}h} - 1\right) - \frac{\partial w}{\partial x} \\ \beta(x,y) &= \frac{E_y h^2}{10G_{yz}}\frac{\partial^3 w}{\partial y^3}\left(\frac{6N_y}{5G_{yz}h} - 1\right) - \frac{\partial w}{\partial y}\end{aligned} \tag{4.20}$$

Substituting Eqs.(4.20) into Eq.(4.16), performing the required differentiation, and algebraically rearranging results in Eq.(4.21). It is the general form of the potential energy expression for a specially orthotropic plate under in-plane compression, including transverse shear deformation.

Eq.(4.21) can now be used to determine the buckling load for a plate with given boundary conditions. The first step is to chose a suitable function for the lateral displacement, w(x,y), which satifies the boundary conditions of the plate. Taking the appropriate derivatives of w(x,y), substituting them into Eq.(4.21), integrating the equation, and taking the variations with respect to the amplitude coefficient, results in a quadratic equation, which set equal to

$$
\begin{aligned}
\psi = \int_0^a \int_0^b \Bigg\{ & -\frac{N_x}{2}\left(\frac{\partial w}{\partial x}\right)^2 - \frac{N_y}{2}\left(\frac{\partial w}{\partial y}\right)^2 + 2D_{xy}\left(\frac{\partial^2 w}{\partial x \partial y}\right)^2 \\
& - 2D_{xy}\frac{E_x h^2}{10G_{xz}}\left(\frac{6N_x}{5G_{xz}h} - 1\right)\frac{\partial^4 w}{\partial x^3 \partial y}\frac{\partial^2 w}{\partial x \partial y} \\
& - 2D_{xy}\frac{E_y h^2}{10G_{yz}}\left(\frac{6N_y}{5G_{yz}h} - 1\right)\frac{\partial^4 w}{\partial x \partial y^3}\frac{\partial^2 w}{\partial x \partial y} \\
& + \frac{D_{xy}}{2}\left[\frac{E_x h^2}{10G_{xz}}\left(\frac{6N_x}{5G_{xz}h} - 1\right)\frac{\partial^4 w}{\partial x^3 \partial y} + \frac{E_y h^2}{10G_{yz}}\left(\frac{6N_y}{5G_{yz}h} - 1\right)\frac{\partial^4 w}{\partial x \partial y^3}\right]^2 \\
& + \frac{D_x}{2}\left[\frac{E_x h^2}{10G_{xz}}\left(\frac{6N_x}{5G_{xz}h} - 1\right)\frac{\partial^4 w}{\partial x^4} - \frac{\partial^2 w}{\partial x^2}\right]^2 \\
& + D_x \nu_{yx}\left[\frac{E_x h^2}{10G_{xz}}\left(\frac{6N_x}{5G_{xz}h} - 1\right)\frac{\partial^4 w}{\partial x^4} - \frac{\partial^2 w}{\partial x^2}\right] \\
& \times \left[\frac{E_y h^2}{10G_{yz}}\left(\frac{6N_y}{5G_{yz}h} - 1\right)\frac{\partial^4 w}{\partial y^4} - \frac{\partial^2 w}{\partial y^2}\right] \\
& + \frac{D_y}{2}\left[\frac{E_y h^2}{10G_{yz}}\left(\frac{6N_y}{5G_{yz}h} - 1\right)\frac{\partial^4 w}{\partial y^4} - \frac{\partial^2 w}{\partial y^2}\right]^2 \\
& + \frac{5}{1200}\frac{E_x^2 h^5}{G_{xz}}\left(\frac{6N_x}{5G_{xz}h} - 1\right)^2\left(\frac{\partial^3 w}{\partial x^3}\right)^2 \\
& + \frac{5}{1200}\frac{E_y^2 h^5}{G_{yz}}\left(\frac{6N_y}{5G_{yz}h} - 1\right)^2\left(\frac{\partial^3 w}{\partial y^3}\right)^2 \Bigg\}\, dydx
\end{aligned}
\tag{4.21}
$$

$$
D_{xy} = \frac{G_{xy} h^3}{12} \tag{4.22}
$$

zero, can be solved for the buckling load. Examples of these solutions for plates with various boundary conditions can be found in the text by Vinson and Chou.

For this analysis, consider the case of a plate with a compressive in-plane load, N_x, acting on the simply supported x-edge with no load acting on the clamped y-edge. A suitable function for the lateral displacement is

$$w(x,y) = A_{mn} \sin\frac{m\pi x}{a}\left[1 - \cos\frac{2n\pi y}{b}\right] \tag{4.23}$$

where A_{mn} is the undetermined amplitude. Substituting the appropriate derivatives of Eq.(4.23) into Eq.(4.21), performing the integration, taking the variation with respect to A_{mn}, and setting the result equal to zero yields Eq.(4.24), a quadratic equation which can be solved for the buckling load.

$$A\bar{N}_x^2 + B\bar{N}_x + C \tag{4.24}$$

where

$$A = \left[\frac{3\pi^2}{500}\left(\frac{G_{xy}}{G_{xz}}\right)\left(\frac{E_x}{G_{xz}}\right)^2\left(\frac{a}{b}\right)^2 n^2 + \frac{9\pi^2}{2000\bar{\nu}}\left(\frac{E_x}{G_{xz}}\right)^3 m^2 + \frac{9}{200}\left(\frac{E_x}{G_{xz}}\right)^2\left(\frac{a}{h}\right)^2\right] \tag{4.25}$$

$$\begin{aligned} B = \Bigg[& -\frac{15}{4\pi^2}\left(\frac{a}{h}\right)^6\frac{1}{m^4} + \frac{\pi^2}{5}\left(\frac{G_{xy}}{G_{xz}}\right)\left(\frac{E_x}{G_{xz}}\right)\left(\frac{a}{b}\right)^2\frac{n^2}{m^2} \\ & - \frac{\pi^4}{100}\left(\frac{G_{xy}}{G_{xz}}\right)\left(\frac{E_x}{G_{xz}}\right)^2\left(\frac{a}{b}\right)^2 n^2 - \frac{\pi^4}{25}\left(\frac{G_{xy}}{G_{xz}}\right)\left(\frac{E_x}{G_{xz}}\right)\left(\frac{E_y}{G_{yz}}\right)\left(\frac{a}{b}\right)^4\frac{n^4}{m^2} \\ & - \frac{3\pi^4}{400\bar{\nu}}\left(\frac{E_x}{G_{xz}}\right)^3 m^2 + \frac{3\pi^2}{40\bar{\nu}}\left(\frac{E_x}{G_{xz}}\right)\left(\frac{a}{h}\right)^2(1-\bar{\nu}) \\ & - \frac{\pi^4}{25\bar{\nu}}\nu_{xy}\left(\frac{E_x}{G_{xz}}\right)^2\left(\frac{E_y}{G_{yz}}\right)\left(\frac{a}{b}\right)^4\frac{n^4}{m^2} + \frac{\pi^2}{10\bar{\nu}}\nu_{xy}\left(\frac{E_x}{G_{xz}}\right)^2\left(\frac{a}{b}\right)^2\left(\frac{a}{h}\right)^2\frac{n^2}{m^2}\Bigg] \end{aligned} \tag{4.26}$$

$$
\begin{aligned}
C = \Bigg[& \frac{5\pi^2}{3}\left(\frac{G_{xy}}{G_{xz}}\right)\left(\frac{a}{b}\right)^2\left(\frac{a}{h}\right)^4\frac{n^2}{m^4} - \frac{\pi^4}{6}\left(\frac{G_{xy}}{G_{xz}}\right)\left(\frac{E_x}{G_{xz}}\right)\left(\frac{a}{b}\right)^2\left(\frac{a}{h}\right)^2\frac{n^2}{m^2} \\
& - \frac{2\pi^4}{3}\left(\frac{G_{xy}}{G_{xz}}\right)\left(\frac{E_y}{G_{yz}}\right)\left(\frac{a}{b}\right)^4\left(\frac{a}{h}\right)^2\frac{n^4}{m^4} + \frac{\pi^6}{240}\left(\frac{G_{xy}}{G_{xz}}\right)\left(\frac{E_x}{G_{xz}}\right)^2\left(\frac{a}{b}\right)^2 n^2 \\
& + \frac{\pi^6}{30}\left(\frac{G_{xy}}{G_{xz}}\right)\left(\frac{E_x}{G_{xz}}\right)\left(\frac{E_y}{G_{yz}}\right)\left(\frac{a}{b}\right)^4\frac{n^4}{m^2} + \frac{\pi^6}{15}\left(\frac{G_{xy}}{G_{xz}}\right)\left(\frac{E_y}{G_{yz}}\right)^2\left(\frac{a}{b}\right)^6\frac{n^6}{m^4} \\
& + \frac{\pi^6}{320\bar{\nu}}\left(\frac{E_x}{G_{xz}}\right)^3 m^2 - \frac{\pi^4}{16\bar{\nu}}\left(\frac{E_x}{G_{xz}}\right)^2\left(\frac{a}{h}\right)^2 + \frac{5\pi^2}{16\bar{\nu}}\left(\frac{E_x}{G_{xz}}\right)\left(\frac{a}{h}\right)^4\frac{1}{m^2} \\
& + \frac{\pi^6}{30\bar{\nu}}\nu_{yx}\left(\frac{E_x}{G_{xz}}\right)^2\left(\frac{E_y}{G_{yz}}\right)\left(\frac{a}{b}\right)^4\frac{n^4}{m^2} - \frac{\pi^4}{12\bar{\nu}}\nu_{yx}\left(\frac{E_x}{G_{xz}}\right)^2\left(\frac{a}{b}\right)^2\left(\frac{a}{h}\right)^2\frac{n^2}{m^2} \\
& - \frac{\pi^4}{3\bar{\nu}}\nu_{yx}\left(\frac{E_x}{G_{xz}}\right)\left(\frac{E_y}{G_{yz}}\right)\left(\frac{a}{b}\right)^4\left(\frac{a}{h}\right)^2\frac{n^4}{m^4} + \frac{5\pi^2}{6\bar{\nu}}\nu_{yx}\left(\frac{E_x}{G_{xz}}\right)\left(\frac{a}{b}\right)^2\left(\frac{a}{h}\right)^4\frac{n^2}{m^4} \\
& + \frac{\pi^4}{32}\left(\frac{E_x}{G_{xz}}\right)^2\left(\frac{a}{h}\right)^2 + \frac{4\pi^6}{15\bar{\nu}}\frac{\nu_{yx}}{\nu_{xy}}\left(\frac{E_x}{G_{xz}}\right)\left(\frac{E_y}{G_{yz}}\right)^2\left(\frac{a}{b}\right)^8\frac{n^8}{m^6} \\
& - \frac{4\pi^4}{3\bar{\nu}}\frac{\nu_{yx}}{\nu_{xy}}\left(\frac{E_x}{G_{xz}}\right)\left(\frac{E_y}{G_{yz}}\right)\left(\frac{a}{b}\right)^6\left(\frac{a}{h}\right)^2\frac{1}{m^6} + \frac{5\pi^2}{3\bar{\nu}}\frac{\nu_{yx}}{\nu_{xy}}\left(\frac{E_x}{G_{xz}}\right)\left(\frac{a}{b}\right)^4\left(\frac{a}{h}\right)^4\frac{n^4}{m^6} \\
& + \frac{2\pi^4}{3}\frac{\nu_{yx}}{\nu_{xy}}\left(\frac{E_x}{G_{xz}}\right)\left(\frac{E_y}{G_{yz}}\right)\left(\frac{a}{b}\right)^6\left(\frac{a}{h}\right)^2\frac{n^6}{m^6}\Bigg]
\end{aligned}
\tag{4.27}
$$

$$
\bar{N}_x = \frac{N_x\pi^2}{G_{xz}h} \quad , \quad \bar{\nu} = 1 - \nu_{xy}\nu_{yx} \tag{4.28}
$$

CHAPTER 5

EFFECTS OF FIBER VOLUME FRACTION ON PLATE STABILITY

Introduction

The equations developed in Chapters Three and Four predict the mechanical properties of a composite plate and its buckling loads. These equations form the mathematical model needed to analyze the effect of fiber volume fraction on a plate's elastic stability. A computer program, listed in the Appendix, was used to calculate the physical properties of a plate using the Halpin-Tsai equations. Once the elastic properties of the plate were determined from the properties of its constituent materials, the program then calculated the buckling load for the plate's given geometry. For comparison purposes, buckling loads for a series of plates with various fiber volume fractions, plate thicknesses, and aspect ratios were computed.

Analysis

The composite plates analyzed were assumed to be made of boron-epoxy material. Typical values for the elastic properties of boron fibers and epoxy resin were used for the analysis. These values are listed in Table 5-1. The only constituent property allowed to vary in predicting the material properties of the plates was the fiber volume fraction. Table 5-2 lists the plate material properties predicted by the computer program for the volume fractions considered. As one would expect, the material's stiffness increased as more fibers were used for reinforcement. However, it should be kept in mind that there are practical limits to this trend. At extreme values of fiber volume fraction ($V_F > 0.75$), factors such as voids in the matrix and contiguity of the fibers can result in premature fracturing of the composite material.

TABLE 5-1. Elastic Properties of Constituent Materials.

Material Property	Boron Fiber	Epoxy Resin
Young's Modulus	60×10^6 psi	$.5 \times 10^6$ psi
Shear Modulus	25×10^6 psi	$.185 \times 10^6$ psi
Poisson's Ratio	0.2	0.35

TABLE 5-2. Elastic Properties of Boron-Epoxy Plates.

Elastic Properties	V_F			
	0.4	0.5	0.6	0.7
E_x (Mpsi)	24.3	30.25	36.2	42.15
E_y (Mpsi)	1.461	1.945	2.776	4.819
G_{xy}, G_{xz} (Mpsi)	0.426	0.551	0.782	1.439
G_{yz} (Mpsi)	0.609	0.811	1.157	2.008
ν_{xy}	0.29	0.275	0.26	0.245
ν_{yx}	0.0174	0.0177	0.0199	0.028

The volume fractions chosen for comparison were V_F = 0.4, 0.5, 0.6, and 0.7. This range represents the practical limits of most realistic composite materials. In many commercially available boron-epoxy tapes, the boron filaments occupy about 50% of the composite volume (DeBolt, 1982). Therefore, the volume fraction V_F = 0.5 was used as a basis to compare with the others.

The geometric properties of the plates were chosen to represent practical systems as well. Values used for the thickness, h, were one-fourth, one-third, and one-half inches. These values kept the composite laminates within the regime of thin plates. The aspect ratio was allowed to vary continuously from A/B equaling one-half to four. This provided a range over which four buckling modes occurred.

Results

Results of the buckling analysis of the composite plates are presented in Figures 5-1 through 5-3. The buckling loads are shown as a function of plate aspect ratio. The inflection points in the curves represent transitions from one longitudinal buckling mode to the next. It is observed from the buckling equation that the minimum buckling load will occur in the first transverse mode. Curves for the different fiber volume fractions are graphed together to show two important trends. The first is that increasing the fiber content of a composite plate results in increasing its buckling load. The second is that as the fiber volume goes up the fibers become increasingly more effective in raising the buckling load.

Tables 5-3 through 5-5 show numerical buckling load data for several specific plate geometries. This data was used to examine how effective changing the fiber volume fraction in the composite was in changing the corresponding buckling load. The results are presented in Tables 5-6 through 5-8. Here, the volume fraction V_F = 0.5 was used as a basis to compare with the other volume fractions.

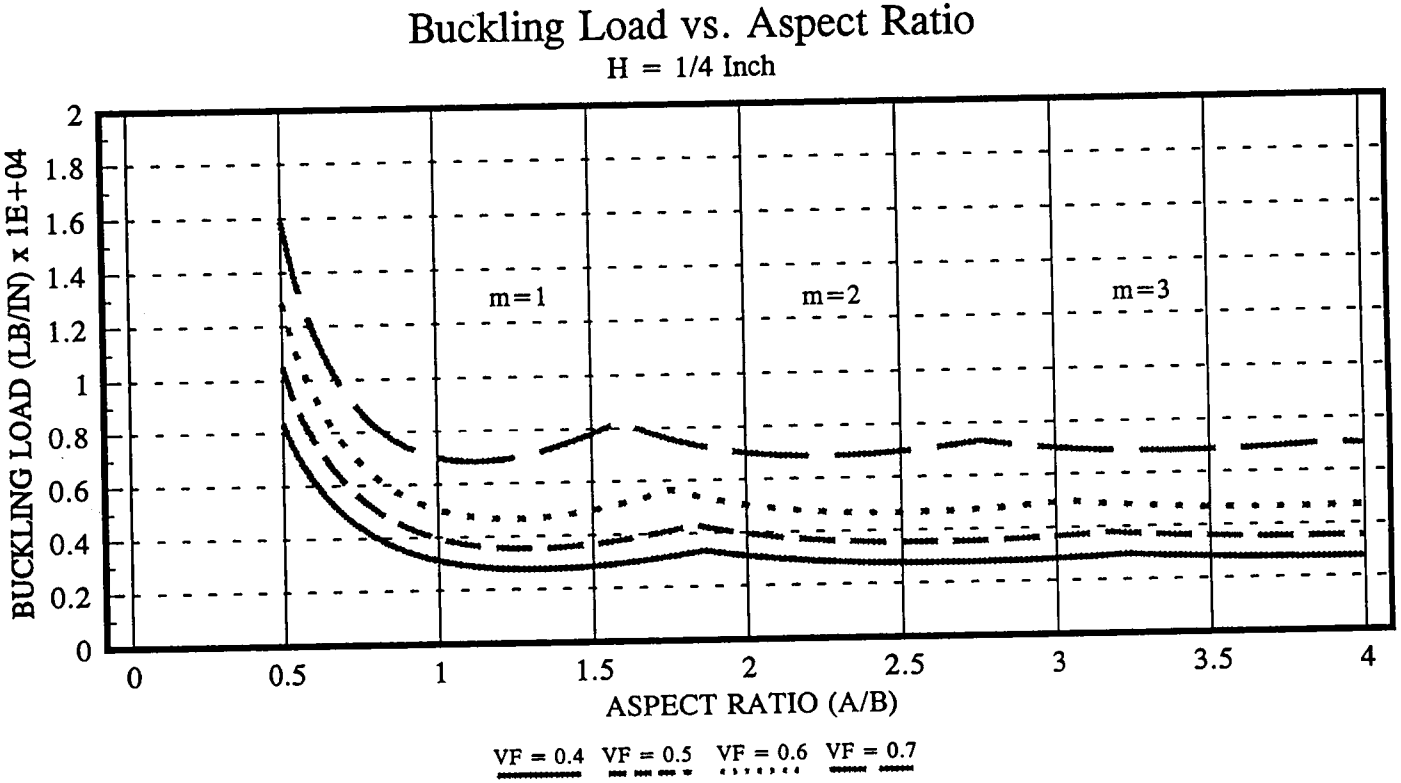


Figure 5-1. Buckling Load vs. Aspect Ratio for Boron-Epoxy Plates 1/4 Inch Thick.

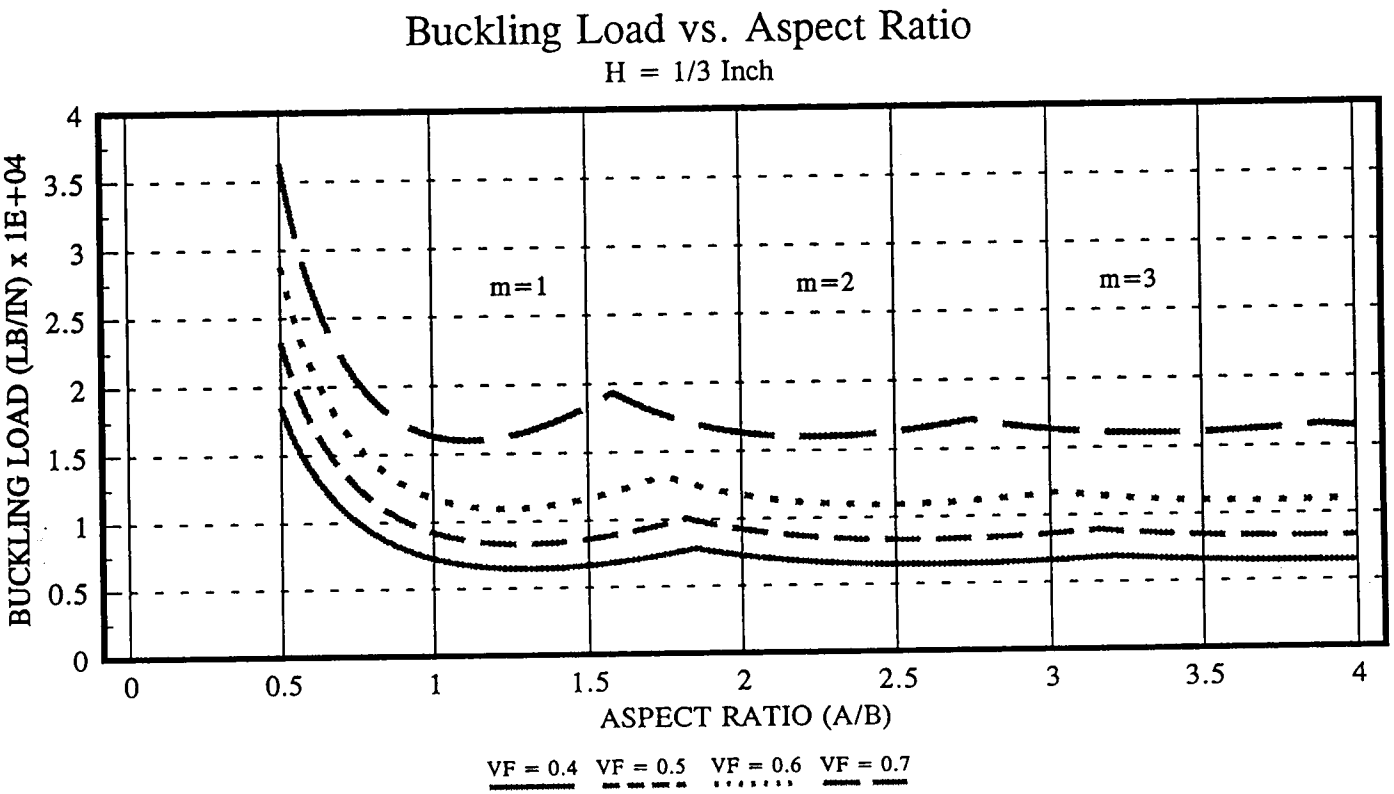


Figure 5-2. Buckling Load vs. Aspect Ratio for Boron-Epoxy Plates 1/3 Inch Thick.

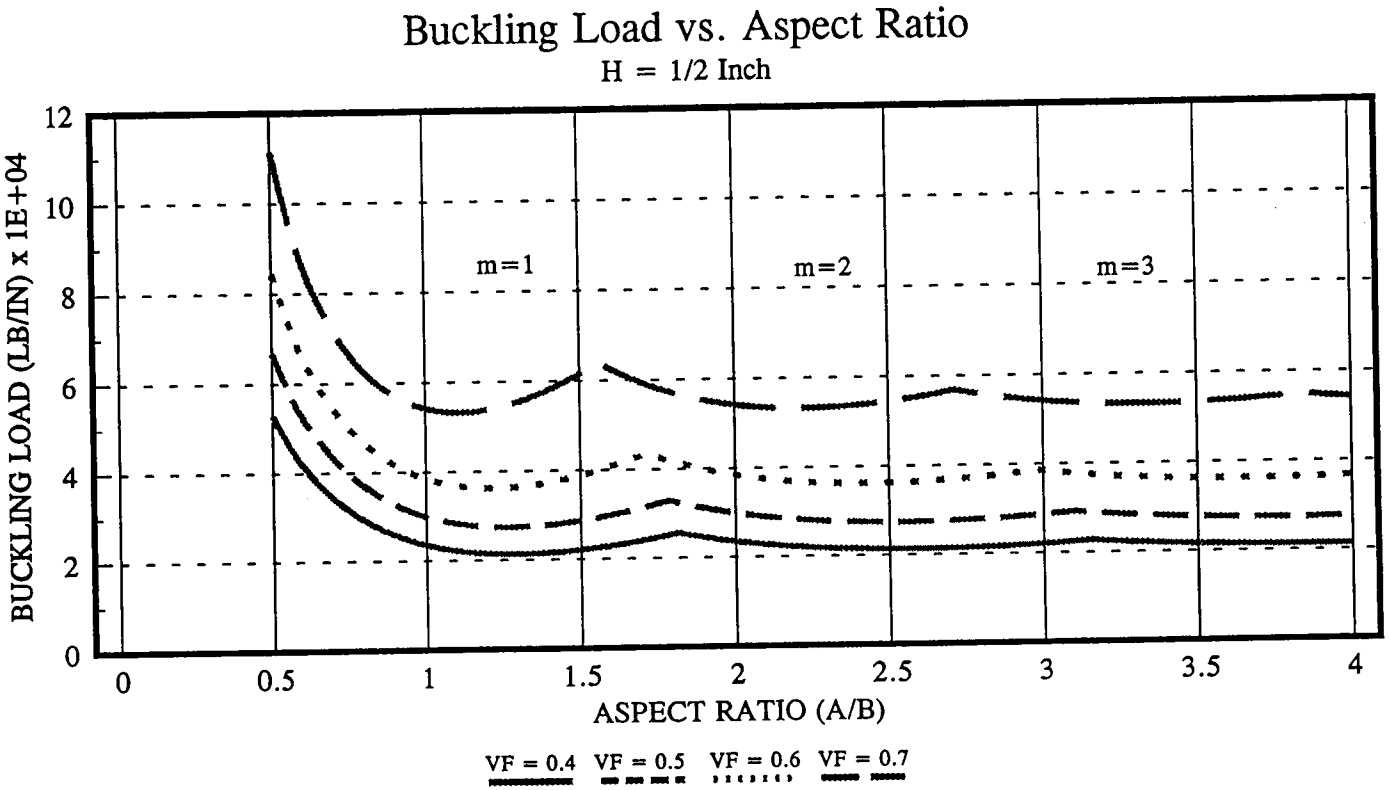


Figure 5-3. Buckling Load vs. Aspect Ratio for Boron-Epoxy Plates 1/2 Inch Thick.

TABLE 5-3. Buckling Loads for Boron-Epoxy Plates 1/4 Inch Thick.
N_x x 1.0E+04

A/B	V_F			
	0.4	0.5	0.6	0.7
1	0.3119	0.3957	0.5039	0.6992
2	0.3119	0.3957	0.5039	0.6992
3	0.2824	0.3663	0.4945	0.6992
4	0.2746	0.3537	0.4695	0.6992

TABLE 5-4. Buckling Loads for Boron-Epoxy Plates 1/3 Inch Thick.
N_x x 1.0E+04

A/B	V_F			
	0.4	0.5	0.6	0.7
1	0.7259	0.9215	1.1763	1.6393
2	0.7259	0.9215	1.1763	1.6393
3	0.6635	0.8609	1.1629	1.6393
4	0.644	0.8299	1.1027	1.6393

TABLE 5-5. Buckling Loads for Boron-Epoxy Plates 1/2 Inch Thick.
N_x x 1.0E+04

A/B	V_F			
	0.4	0.5	0.6	0.7
1	2.3552	2.9951	3.8481	5.4261
2	2.3552	2.9951	3.8481	5.4261
3	2.2097	2.8686	3.8481	5.4261
4	2.1343	2.7529	3.6678	5.4261

Tables 5-6 through 5-8 show that reducing fiber volume by 20%, from $V_F = 0.5$ to $V_F = 0.4$, results in a 21% to 23% reduction in the buckling load. Increasing fiber volume by 20%, from $V_F = 0.5$ to $V_F = 0.6$, however, increases the buckling load by 27% to 35%. A 40% increase in fiber volume, from $V_F = 0.5$ to $V_F = 0.7$, raises the buckling load approximately 77% to 98%.

The numbers in Tables 5-6 through 5-8 verify the trends observed from Figures 5-1 through 5-3 concerning the effects of altering the fiber content of the composites. Increasing the fiber volume of a composite plate does increase its elastic stability. This is particularly true for plates with higher aspect ratios. For plates with aspect ratio equal to four, a 40% increase in fibers effectively doubles the buckling load. Figure 5-4 shows the percentage change in the buckling load as a function of the volume fraction. The chart is graphed with the average percentage change for each of the aspect ratios considered. Clearly, the fiber volume fraction is an important parameter to be considered in designing composite plates to withstand compression.

TABLE 5-6. Percentage Change in Buckling Loads for Boron- Epoxy Plates 1/4 Inch Thick. Based on $V_F = 0.5$

A/B	V_F		
	0.4	0.6	0.7
1	-21.2%	27.3%	76.7%
2	-21.2%	27.3%	76.7%
3	-22.9%	35.0%	90.9%
4	-22.4%	32.7%	97.7%

TABLE 5-7. Percentage Change in Buckling Loads for Boron- Epoxy Plates 1/3 Inch Thick. Based on $V_F = 0.5$

A/B	V_F		
	0.4	0.6	0.7
1	-21.2%	27.7%	77.9%
2	-21.2%	27.7%	77.9%
3	-22.9%	35.1%	90.4%
4	-22.4%	32.9%	97.5%

TABLE 5-8. Percentage Change in Buckling Loads for Boron- Epoxy Plates 1/2 Inch Thick. Based on $V_F = 0.5$

A/B	V_F		
	0.4	0.6	0.7
1	-21.4%	28.5%	81.2%
2	-21.4%	28.5%	81.2%
3	-23.0%	34.1%	89.2%
4	-22.5%	33.2%	97.1%

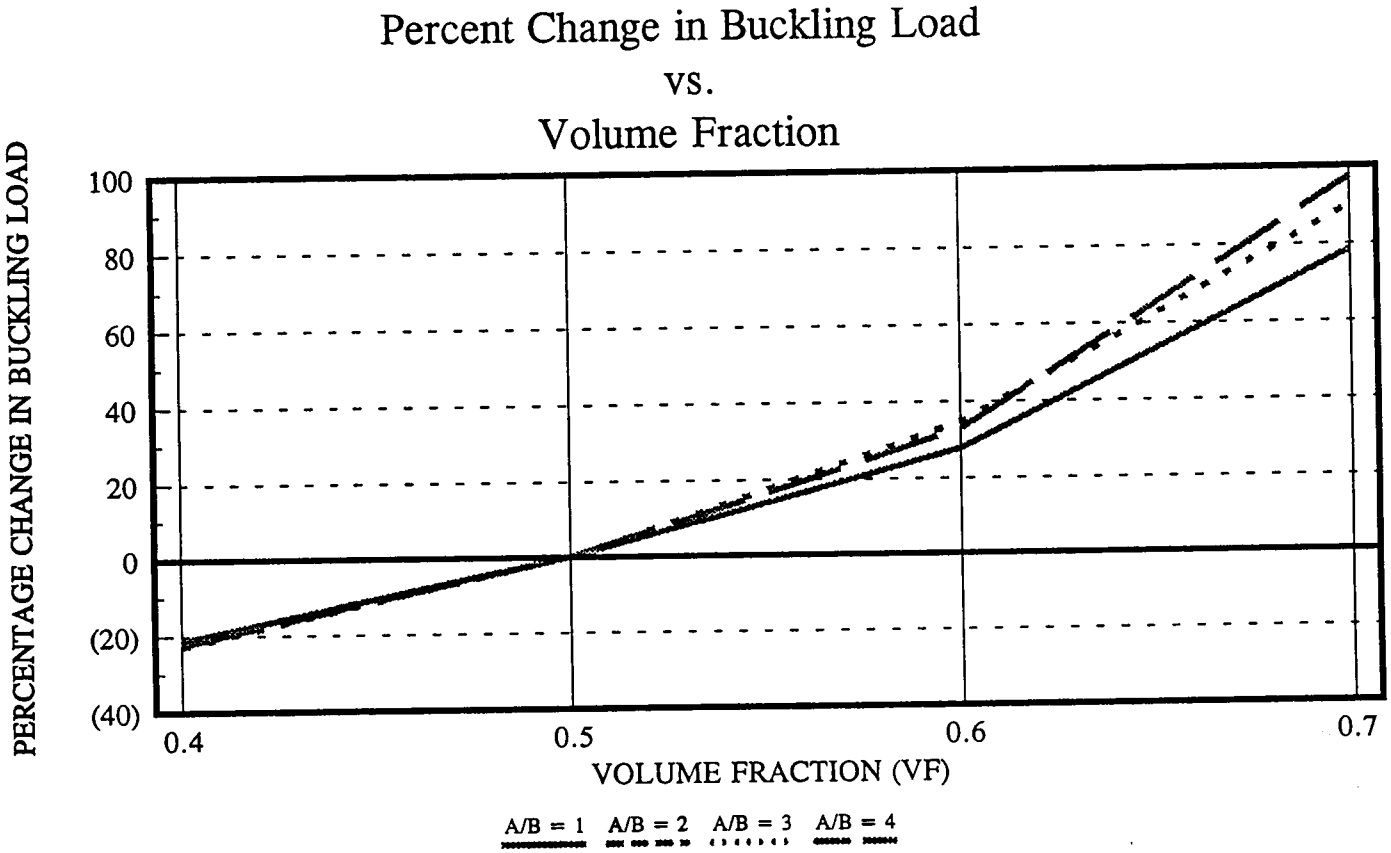


Figure 5-4. Percentage Change in Buckling Load vs. Volume Fraction.

CHAPTER 6

CONCLUSIONS AND RECOMMENDATIONS

Advanced composite materials, such as boron-epoxy, possess tremendous potential to further the state of the art in aerospace structures. Because of their high-strength, high-stiffness, and low weight properties, compared to conventional structural materials, composite structures can substantially enhance the performance capabilities of modern aircraft and space vehicles.

Composites have been successfully used for many years in the design and development of a variety of flight vehicle components. Weight reductions up to 50% have been achieved in these types of structures. Before composites can be used to their maximum potential, however, it will be necessary to systematically incorporate them into every structural component within the airframe.

The analysis of composite aircraft structures can be broken down into the general categories of micromechanics, macromechanics, and structural analysis. This investigation has combined two of those categories, namely micromechanics and structural analysis, to analyze the relationship between one of a composite material's constituent properties and its overall structural integrity. The analysis used micromechanics theory, in the form of the Halpin-Tsai equations, to calculate the material properties of a composite plate from the properties of its constituents. Once these values were known, they were incorporated into a buckling equation developed from Reissner's variational theorem. Because the shear modulus of unidirectional composites is relatively low in comparison to its high axial stiffness, shear effects must be considered in compression stability analysis. This stability analysis used a buckling equation that included transverse shear effects. Results of this investigation show that

increasing the fiber volume fraction of a composite plate dramatically increases its ability to withstand compressive loads.

It must be remembered that the results obtained are for a specific composite material, that is boron-epoxy. Boron fibers have extremely high stiffness and strength properties. Therefore, it cannot be presumed that increasing the fiber volume fraction of other composite materials will increase their buckling load capacity as dramatically as was seen here. It may be concluded, however, that increasing the fiber content of a composite material will increase its elastic stability to some extent. The methodology used in this investigation is applicable to any unidirectional composite material which can be classified as specially orthotropic and transversely isotropic. The trends observed for boron-epoxy are therefore valid for any continuous fiber filament embedded in an epoxy matrix.

Recommendations for further study include using this technique to analyze the effects altering other constituent properties has on the elastic stability of composite plates. By holding all constituent properties constant, except the one being investigated, an understanding of its particular influence on the buckling load could be obtained.

Another area of interest might be to incorporate macromechanics into the analysis, and investigate the area of angle ply laminates. Trade-off studies could be performed to determine the optimal use of constituent materials, ply directions and lay-up schemes for a given load bearing capacity. This type of analysis would allow designers to develop composite structures meeting elastic stability requirements in the most efficient manner possible.

BIBLIOGRAPHY

BIBLIOGRAPHY

Adams, Donald F. and Douglas R. Doner, "Transverse Normal Loading of a Unidirectional Composite," Journal of Composite Materials, **1**, 152, April, 1967.

Adams, Donald F. and Douglas R. Doner, "Longitudinal Shear Loading of a Unidirectional Composite," Journal of Composite Materials, **1**, 4, January, 1967.

Agarwal, Bhagwan D. and Lawrence J. Broutman, Analysis and Performance of Fiber Composites, Second Edition, John Wiley & Sons, Inc., 1990.

Ambartsumyan, S.A., Theory of Anisotropic Plates, Technomic Publishing Co., 1970.

Ashton, J.E., "Anisotropic Plate Analysis-Boundary Conditions," Journal of Composite Materials, **4**, 162, April, 1970.

Beer, Ferdinand P. and E. Russell Johnston, Jr., Mechanics of Materials, McGraw-Hill Book Co., 1981.

Calcote, Lee R., The Analysis of Laminated Composite Structures, Van Nostrand Reinhold Co., 1969.

Chen, Paul E., "Bending and Buckling of Anisotropic Plates," S.W. Tsai, J.C. Halpin, N.J. Pagano, Eds., Composite Materials Workshop, Technomic Publishing Co., 1968.

Christensen, R.M., Mechanics of Composite Materials, John Wiley & Sons, Inc., 1979.

DeBolt, Harold E., "Boron and Other High-Strength, High-Modulus, Low-Density Filamentary Reinforcing Agents," George Lubin , Ed., Handbook of Composites, Van Nostrand Reinhold Co., 1982.

Hadcock, R.N., "Boron-Epoxy Aircraft Structures," George Lubin, Ed., Handbook of Fiberglass and Advanced Plastics Composites, Van Nostrand Reinhold Co., 1969.

Hadcock, R.N., "Design and Analysis of Advanced Composite Structures," George Lubin , Ed., Handbook of Composites, Van Nostrand Reinhold Co., 1982.

Hahn, H. Thomas and Jerry G. Williams, "Compression Failure Mechanisms in Unidirectional Composites," NASA Technical Memorandum 85834, August, 1984.

Halpin, J.C., Primer on Composite Materials: Analysis, Revised, Technomic Publishing Co., 1984.

Halpin, J.C., "Effects of Environmental Factors on Composite Materials," Technical Report AFML-TR-67-423, June, 1969.

Hermans, J.J., "The Elastic Properties of Fiber Reinforced Materials when the Fibers are Aligned," Proc. Konigl. Nederl. Akad. van Weteschappen Amsterdam, **B70** (1), 1, 1967.

Hewitt, R.L. and M.C. De Malherbe, "An Approximation for the Longitudinal Shear Modulus of Continuous Fibre Composites," Journal of Composite Materials, **4**, 280, April, 1970.

Hill, R., "Theory of Mechanical Properties of Fibre-Strengthened Materials-III. Self-Consistent Model," J. Mech. Phys. Solids, **13**, 189, 1965.

Jones, Robert M., Mechanics of Composite Materials, Scripta Book Co., 1975.

June, R.R. and J.R. Lager, "Commercial Aircraft," M.J. Salkind and G.S. Holister, Eds., Applications of Composite Materials, STP 524, American Society for Testing and Materials, 1973.

Lekhnitskii, S.G., Theory of Elasticity of an Anisotropic Elastic Body, Holden-Day Inc., 1963.

Linsenmann, Don R., "Stability of Plates of Composite Materials," MMAE Thesis, University of Delaware, 1974.

Lubin, George and Samuel J. Dastin, "Aerospace Applications of Composites," George Lubin, Ed., Handbook of Composites, Van Nostrand Reinhold Co., 1982.

Masters, John E., "Basic Failure Modes of Continuous Fiber Composites," Engineered Materials Handbook, Volume 1, Composites, ASM International, Third Printing, August, 1989.

Pagano, N.J. and S.W. Tsai, "Micromechanics of Composite Media," S.W. Tsai, J.C. Halpin, N.J. Pagano, Eds., Composite Materials Workshop, Technomic Publishing Co., 1968.

Penn, Lynn S. and T.T. Chiao, "Epoxy Resins", George Lubin , Ed., Handbook of Composites, Van Nostrand Reinhold Co., 1982.

Rosato, Dominick V., "An Overview of Composites," George Lubin, Ed., Handbook of Composites, Van Nostrand Reinhold Co., 1982.

Reissner, Eric, "On a Variational Theorem in Elasticity," Journal of Math. and Phys., **29**, 90, 1950.

Rosen, Walter B. and Norris F. Dow, "Overview of Composite Materials Analysis and Design," Engineered Materials Handbook, Volume 1, Composites, ASM International, Third Printing, August, 1989.

Rosen, Walter B., "Analysis of Material Properties," Engineered Materials Handbook, Volume 1, Composites, ASM International, Third Printing, August, 1989.

Smith, Alton P., Jr, "The Effect of Transverse Shear Deformation on the Elastic Stability of Orthotropic Plates Due to Inplane Loads," MMAE Thesis, University of Delaware, 1973.

Tsai, Stephen W. and H. Thomas Hahn, Introduction to Composite Materials, Technomic Publishing Co., 1980.

Timoshenko, Stephen P. and James M. Gere, Theory of Elastic Stability, Second Edition, McGraw-Hill Book Co., 1961.

Vinson, Jack R. and Tsu-Wei Chou, Composite Materials and Their Use in Structures, Halsted Press, 1975.

Whitney, James M., "Analytical and Experimental Methods in Composite Mechanics," Journal of the Structural Division, Proceedings of the American Society of Civil Engineers, Vol. 99, No. ST1, January, 1972.

Whitney, James M., "The Effect of Transverse Shear Deformation on the Bending of Laminated Plates," Journal of Composite Materials, **3**, 534, July, 1969.

Whitney, James M., "The Effect of Boundary Conditions on the Response of Laminated Composites," Journal of Composite Materials, **4**, 192, April, 1970.

APPENDIX

APPENDIX

```
OPEN "BUCK1.TXT" FOR OUTPUT AS #1 LEN = 512
OPEN "BUCK2.TXT" FOR OUTPUT AS #2 LEN = 512
OPEN "BUCK3.TXT" FOR OUTPUT AS #3 LEN = 512
CLS : DIM QQ(4), HH(3)
HH(1) = .25: HH(2) = .333: HH(3) = .5

'Material Properties of the Lamina Constituents

EF = 6E+07: NUF = .2: GF = 2.5E+07
EM = 500000: NUM = .35: GM = 185000

'Halpin-Tsai Equations

FOR J = 1 TO 3 STEP 1
FOR I = .4 TO .8 STEP .1
VF = I
VM = 1 - VF
ZTAG = 1 + 40 * VF ^ 10
ZTAE = 2 + 40 * VF ^ 10
EX = EF * VF + EM * VM
NUXY = NUF * VF + NUM * VM
ETAG = (GF / GM - 1) / (GF / GM + ZTAG)
ETAE = (EF / EM - 1) / (EF / EM + ZTAE)
EY = ((1 + ZTAE * ETAE * VF) / (1 - ETAE * VF)) * EM
NUYX = NUXY * EY / EX
NUYZ = (1 - ETAG) / (1 - ETAE) * (1 + ETAE * ZTAE) / (1 + ETAG * ZTAG) * (EM / (2 *
GM)) - 1
GXY = ((1 + ZTAG * ETAG * VF) / (1 - ETAG * VF)) * GM
GXZ = GXY
GYZ = EY / (2 * (1 + NUYZ))

'Define Ratios used in the Buckling Equation

FOR AB = .5 TO 4 STEP .01
FOR M = 1 TO 4 STEP 1
PI = 3.14159: PI2 = PI ^ 2: PI4 = PI ^ 4: PI6 = PI ^ 6
N = 1: M2 = M ^ 2: M4 = M ^ 4: M6 = M ^ 6
B = 1: A = AB * B: AB2 = AB ^ 2: AB4 = AB ^ 4: AB6 = AB ^ 6
AB8 = AB ^ 8
H = HH(J): AH = A * 12 / H: AH2 = AH ^ 2: AH4 = AH ^ 4
AH6 = AH ^ 6
N2M2 = N / M2: N4M2 = N / M2: N2M4 = N / M4: N4M4 = N / M4
N6M4 = N / M4
N8M6 = N / M6: N4M6 = N / M6: N6M6 = N / M6
NUBR = 1 - NUXY * NUYX: YXXY = NUYX / NUXY
GXYZ = GXY / GXZ: EGYZ = EY / GYZ: EGYZ2 = EGYZ ^ 2
```

```
EGXZ = EX / GXZ: EGXZ2 = EGXZ ^ 2: EGXZ3 = EGXZ ^ 3

'Solve the Coefficients of the Buckling Equation

C11 = 3 * PI2 / 500 * GXYZ * EGXZ2 * AB2 * N ^ 2
C12 = 9 * PI2 / (2000 * NUBR) * EGXZ3 * M2
C13 = 9 / 200 * EGXZ2 * AH2
C1# = C11 + C12 + C13

C21 = -15 / (4 * PI2) * AH6 / M4
C22 = PI2 / 5 * GXYZ * EGXZ * AB2 * N2M2
C23 = -PI4 / 100 * GXYZ * EGXZ2 * AB2 * N ^ 2
C24 = -PI4 / 25 * GXYZ * EGXZ * EGYZ * AB4 * N4M2
C25 = -3 * PI4 / (400 * NUBR) * EGXZ3 * M2
C26 = 3 * PI2 / (40 * NUBR) * EGXZ * AH2 * (1 - NUBR)
C27 = -PI4 / (25 * NUBR) * NUYX * EGXZ2 * EGYZ * AB4 * N4M2
C28 = PI2 / (10 * NUBR) * NUYX * EGXZ2 * AB2 * AH2 * N2M2
C2# = C21 + C22 + C23 + C24 + C25 + C26 + C27 + C28

C31 = 5 * PI2 / 3 * GXYZ * AB2 * AH4 * N2M4
C32 = -PI4 / 6 * GXYZ * EGXZ * AB2 * AH2 * N2M2
C33 = -2 * PI4 / 3 * GXYZ * EGYZ * AB4 * AH2 * N4M4
C34 = PI6 / 240 * GXYZ * EGXZ2 * AB2 * N ^ 2
C35 = PI6 / 30 * GXYZ * EGXZ * EGYZ * AB4 * N4M2
C36 = PI6 / 15 * GXYZ * EGYZ2 * AB6 * N6M4
C37 = PI6 / (320 * NUBR) * EGXZ3 * M2
C38 = -PI4 / (16 * NUBR) * EGXZ2 * AH2
C39 = 5 * PI2 / (16 * NUBR) * EGXZ * AH4 * 1 / M2
C40 = PI6 / (30 * NUBR) * NUYX * EGXZ2 * EGYZ * AB4 * N4M2
C41 = -PI4 / (12 * NUBR) * NUYX * EGXZ2 * AB2 * AH2 * N2M2
C42 = -PI4 / (3 * NUBR) * NUYX * EGXZ * EGYZ * AB4 * AH2 * N4M4
C43 = 5 * PI2 / (6 * NUBR) * NUYX * EGXZ * AB2 * AH4 * N2M4
C44 = PI4 / 32 * EGXZ2 * AH2
C45 = 4 * PI6 / (15 * NUBR) * YXXY * EGXZ * EGYZ2 * AB8 * N8M6
C46 = -4 * PI4 / (3 * NUBR) * YXXY * EGXZ * EGYZ * AB6 * AH2 * 1 / M6
C47 = 5 * PI2 / (3 * NUBR) * YXXY * EGXZ * AB4 * AH4 * N4M6
C48 = 2 * PI4 / 3 * YXXY * EGXZ * EGYZ * AB6 * AH2 * N6M6
DC3 = C31 + C32 + C33 + C34 + C35 + C36 + C37 + C38 + C39
EC3 = C40 + C41 + C42 + C43 + C44 + C45 + C46 + C47 + C48
C3# = DC3 + EC3

'Solve the Quadratic Equation for the Buckling Load

ROOT# = C2# ^ 2 - 4 * C1# * C3#
NX1# = (-C2# - SQR(ROOT#)) / (2 * C1#)
NX2# = (-C2# + SQR(ROOT#)) / (2 * C1#)
IF NX1# < NX2# THEN NXT# = NX1#
IF NX2# < NX1# THEN NXT# = NX2#
NBAR# = NXT# * GXZ * H / (PI2 * 10000)
QQ(M) = NBAR#
NEXT M
```

```
IF QQ(1) < QQ(2) AND QQ(1) < QQ(3) AND QQ(1) < QQ(4) THEN X = 1
IF QQ(2) < QQ(1) AND QQ(2) < QQ(3) AND QQ(2) < QQ(4) THEN X = 2
IF QQ(3) < QQ(1) AND QQ(3) < QQ(2) AND QQ(3) < QQ(4) THEN X = 3
IF QQ(4) < QQ(1) AND QQ(4) < QQ(2) AND QQ(4) < QQ(3) THEN X = 4
NBAR# = QQ(X)

PRINT "I= "; I; "H= "; H; "M= "; X; "AB= "; AB; "NBAR= "; NBAR#
IF J = 1 THEN PRINT #1, USING "###.#### "; I; H; X; AB; NBAR#
IF J = 2 THEN PRINT #2, USING "###.#### "; I; H; X; AB; NBAR#
IF J = 3 THEN PRINT #3, USING "###.#### "; I; H; X; AB; NBAR#

NEXT AB
NEXT I
NEXT J
END
```

VITA

John Paul McMillan, Jr. was born in Mullins, South Carolina on January 16, 1960. He graduated from Mullins High School in June 1978 and enlisted in the United States Air Force. He served in the 91 Civil Engineering Squadron at Minot AFB, North Dakota from August 1978 until December 1981. At that time he was awarded a four year AFROTC scholarship to attend Mississippi State University. After graduating in December 1985 with a degree in Aerospace Engineering, he was commissioned as a Second Lieutenant into the USAF. He completed Undergraduate Navigator Training at Mather AFB, California, and was assigned to the 15 Military Airlift Squadron at Norton AFB, California where he flew C-141B aircraft for five years. After leaving the military in August of 1990, he entered the University of Tennessee Space Institute, and received a Master of Science degree in Aerospace Engineering in May 1994.